Exploring climate-driven phenological mismatches in pears, pests and natural enemies: a multi-model approach

Journal of Pest Science
https://doi.org/10.1007/s10340-025-01874-6

Exploring climate-driven phenological mismatches in pears, pests and natural enemies: a multi-model approach

Laura A. Reeves[1] · Tim Belien[2] · Deepa Senapathi[1] · Michael P. D. Garratt[1] · Michelle T. Fountain[3]

Received: 21 August 2024 / Revised: 21 January 2025 / Accepted: 24 January 2025

Abstract

Pear psyllid (*Cacopsylla pyri*) is the dominant pest of UK pear orchards, with an estimated cost of £5 million per annum. Insecticide withdrawal and increased pesticide resistance of *C. pyri* have led many growers to depend more on natural enemies for pest management, including earwigs. However, there is concern how phenological events may shift with future climate change, which may result in phenological mismatches. This study aimed to determine shifts in timing of phenological events within an agroecosystem and predict phenological mismatches or synchronies between trophic levels. We evaluated three models: the *C. pyri* phenology model, the earwig degree day model and the PhenoFlex model (flowering time). Phenological events predicted by models included: first, full and last flowering time for *Pyrus communis*; peak psyllid abundance date for first-generation (G1) *C. pyri* nymphs and second-generation (G2) eggs, nymphs and adults; and peak abundance date for stage 4 *Forficula auricularia* and adults. Findings indicated that the timing of phenological events was advancing for all trophic levels, becoming significantly earlier under the current time period. Furthermore, predictions indicated that timing events would continue to advance under the RCP8.5 scenario. However, not all phenological events advanced at the same rate; the date of peak *C. pyri* G1 nymph abundance advanced at a higher rate than full flowering time, which could result in a phenological mismatch by 2071. Conversely, *C. pyri* and *F. auricularia* showed phenological synchrony, with peak abundance dates advancing at a similar rate, which could be beneficial for future biological control.

Keywords Biological control · *Cacopsylla pyri* · Climate change · *Forficula auricularia* · Phenological models · Multi-trophic interactions

Introduction

There are over 4000 described species of psyllid globally (Mauck et al. 2024) and 24 known species of pear psyllid (*Pyrus* spp.) (Civolani et al. 2023). *Cacopsylla pyri* is currently the dominant pear psyllid species in the UK and is especially prevalent in Kent, whereas *Cacopsylla pyricola* was previously more abundant during the 1970–1980s (Nagy et al. 2008; Reeves et al. 2024). These phloem feeding insects cause significant damage to orchards: nymphs produce honeydew: a sugary secretion that encourages growth of black sooty mould on fruit and leaves (Daniel et al. 2005), and adults are a vector of the pathogen 'pear decline' (*Candidatus* Phytoplasma pyri), which can reduce shoot and fruit growth and lead to tree death (Carraro et al. 2001; Kucerová et al. 2007; Süle et al. 2007). The pear industry is economically important with 17.9 thousand tonnes of pears produced in the UK (Defra 2023) and 26.3 million tonnes produced globally in 2022 (FAOSTAT 2022); thus, changes to phenology or control of *C. pyri* could have significant economic impact.

Pear psyllids have demonstrated resistance to a range of common pesticides (Erler 2004; Harries and Burts 1965; Sek Kocourek and Stará 2006); furthermore, three insecticides used in pear psyllid management have recently been withdrawn from UK use (Reeves et al. 2024). Thus, integrated pest management (IPM) has become a priority for managing

Communicated by Andrea Battisti.

✉ Laura A. Reeves
l.reeves@pgr.reading.ac.uk

[1] Centre for Agri-Environmental Research, School of Agriculture, Policy and Development, University of Reading, Reading, Berkshire RG6 6AR, UK

[2] Zoology Department, Proefcentrum Fruitteelt vzw, Fruittuinweg 1, 3800 Sint-Truiden, Belgium

[3] NIAB, New Road, East Malling, Kent ME19 6BJ, UK

Published online: 05 February 2025

pear psylla (Reeves et al. 2023; Shaw et al. 2021), maintaining healthy crop growth whilst minimising disruption to agroecosystems, focusing on enhancing biological control (Moorthy and Kumar 2004). There are a wide range of pear psyllid natural enemies (Civolani et al. 2023; Horton 2024). The anthocorid *Anthocoris nemoralis* is a well-documented biocontrol agent of *C. pyri* (Nagy et al. 2008; Sigsgaard 2010). *Anthocoris nemoralis* populations peak during July–August, helping to control *C. pyri* populations (Fields and Beirne 1973; Scutareanu et al. 1999). It has become common practice for growers to mass release *A. nemoralis* into pear orchards (Reeves et al. 2024). In addition, the European earwig *Forficula auricularia* (Linnaeus) is a key natural enemy of pear psylla; stage four earwig nymphs are arboreal, appearing in pear trees in late spring and peaking in June, whilst adult populations peak in mid-July (Gobin et al. 2008; Moerkens et al. 2011). Arboreal *F. auricularia* nymphs can consume up to 1000 psylla eggs a day (Lenfant et al. 1994). Although *F. auricularia* is not commonly reared for mass release, enhancing earwig populations by providing refugia is recommended (Shaw et al. 2021). Other *C. pyri* natural enemies include ladybird adults and larvae (Coccinellidae) (Fountain et al. 2013; Prodanović et al. 2010), lacewing larvae (Neuroptera) (DuPont and Strohm 2020; DuPont et al. 2023), spiders (Araneae) (Petrakova et al. 2016), other anthocorid species (Sigsgaard 2010; Vrancken et al. 2014) and parasitoids (Prodanović et al. 2010; Tougeron et al. 2021).

Cacopsylla pyri overwinter as adults in bark crevices (Næss 2016), during which reproductive diapause occurs (Lyoussoufi et al. 1994; Schaub et al. 2005). By mid-late winter, ovaries are fully developed (Schaub et al. 2005) and egg laying starts in late February (Næss 2016; Oz and Erler 2021). Pear psyllid eggs hatch in early spring, often coinciding with bud opening, and there are five nymphal stages, each ending in a mould (Civolani et al. 2023). The first peak in the pear psyllid population is often seen around April–May, followed by a second generation in early summer (Reeves et al. 2024). Subsequent generations overlap throughout the summer and early autumn (Civolani et al. 2023), with an average of 3–5 generations per year (Süle et al. 2007), although this can be temperature dependent (Kapatos and Stratopoulou 1999).

Climate is predicted to change significantly over the next 80 years globally, whilst UK Climate Projections (UKCP18) predict hotter, drier summers and warmer, wetter winters (Lowe et al. 2018; Murphy et al. 2018). This will likely affect psyllid development and interactions with natural enemies. By 2070, summer temperatures could increase as much as 5.1 °C under the RCP8.5 scenario, whilst becoming up to 45% drier (MetOffice 2022). Representative Concentration Pathways (RCPs) are the concentrations of greenhouse gases that will result in total radiative forcing increasing by a certain threshold by 2100, compared to pre-industrial levels. These scenarios are often used to model how future climate will change with respect to different emissions scenarios, with RCP2.6 (low emissions scenarios) representing a significant reduction in greenhouse gas emissions (Van Vuuren et al. 2011), and RCP8.5 (high emissions scenario) is a 'business-as-usual' scenario where greenhouse gas emissions increase unchecked (MetOffice 2018).

There is concern that climate change could alter trophic interactions and phenological events within agroecosystems (Harrington et al. 1999; Reeves et al. 2024; Renner and Zohner 2018; Wyver et al. 2023). Phenological mismatches are a particular concern for agricultural ecosystems, where shifts in other trophic levels do not match the corresponding shift for pest species (Damien and Tougeron 2019). Phenological synchrony is important within this agroecosystem; whether peak natural enemy abundance corresponds to peak pear psyllid abundance is central to pest management (Reeves et al. 2024). Pear psyllid nymph emergence corresponding with budburst can be beneficial, as they nymphs access fleshly plant tissue when feeding; additionally, flower buds can provide shelter for nymphs from adverse weather conditions, agrochemical sprays and natural enemies (Derksen et al. 2007; Reeves et al. 2022). All three trophic levels (pear, pest and natural enemy) are likely to be influenced by climate change. Pear flowering phenology is influenced by chilling time (the time spent below a certain temperature) and forcing time (the time spent above a certain temperature post-chilling) (Cesaraccio et al. 2004; Drepper et al. 2020). If higher temperatures are experienced during the forcing period, but chilling requirements are still met, earlier flowering is likely. In addition, pear psyllids have temperature-dependent development (McMullen and Jong 1977; Schaub et al. 2005); development rates of nymphs and eggs are linearly dependent on temperature, up to a certain threshold. Higher temperatures are likely to advance pest emergence and could impact voltinism (number of generations per year) (Karuppaiah and Sujayanad 2012). Development rates of *F. auricularia* have a nonlinear response to temperature, as a sigmoidal curve (Moerkens et al. 2011). Therefore, comparing whether pear psyllids and their natural enemies respond to temperature at the same rate is important to understand potential phenological mismatches and future pest control scenarios.

The aim of this study was to: (1) combine the psyllid phenology model developed by Schaub et al. (2005), the Earwig phenological day degree model Moerkens et al. (2011) and the PhenoFlex flowering time model Luedeling (2023), applying the models to UK data to assess whether they are relevant for UK predictions, (2) predict how all three trophic levels (pear, pest and natural enemy) could respond under future temperature scenarios and (3) observe whether all three trophic levels are advancing at the same

rate or whether phenological mismatches are likely. This study provides a multi-trophic approach that can be easily applied to other agroecosystems, highlighting its importance within the scientific literature.

Materials and methods

An overview of the data inputs, outputs and processes used within the paper can be found within the supplementary material (Figure S1).

Long-term pear sucker and natural enemy monitoring data

Long-term pear psyllid and natural enemy data were collected by agronomists from 18 different sites in Kent, UK, between 2011 and 2021. The method used for monitoring pear psyllid and their natural enemies is adapted from Cross and Berrie (2003); 30 trees were sampled in a W distribution across the orchard. Pear psyllid abundance was calculated by using beat tray sampling and collecting leaf material, every week from mid-March to August each year. Adult pear psyllid and natural enemy species: earwigs, ladybirds and anthocorids (nymphs and adults), were monitored using beat tray sampling; a white plastic tray (390 mm by 235 mm) was held underneath a randomly selected tree branch on each tree and total numbers were recorded. For monitoring nymphs and eggs, six rosette and six young shoot leaves were randomly selected; these were examined using a hand lens. When leaves were not present, a bud with 6 cm of the branch underneath was examined. Samples were collected from cv. Conference pear (*Pyrus communis*) orchards. An average abundance of each species (psyllids and natural enemies) and stage (eggs, nymphs and adults) was calculated each week, for each orchard. The peak abundance date was then calculated for each species and stage in each orchard. This is based on the date when average abundance was highest and used as the observed peak abundance date. The size of each orchard did vary, with an average size of 3.24 ha ± 0.57 (SE).

Pear flowering data

Historical data on pear flowering times were collated from 1960 to 2021 at NIAB (formerly East Malling Research, 51.2885° N, 0.4383° E) in Kent, UK (Reeves et al. 2022).

Phenological data on pear flowering were collected for the following metrics:

- First (first flower opens on a tree or anthers are visible),
- Full (50% of flowers have opened on the tree) and
- Last (90% petal fall)

Phenological data were analysed for cv. Conference pear trees (*P. communis*), as this cultivar was present in all orchards used for monitoring. Based on the UK horticulture statistics, Conference pear (*P. communis* cv. Conference) is the most common pear cultivar in the UK (Defra 2023). These data were used to calibrate and validate the PhenoFlex model.

Temperature data and future scenarios

Hourly air temperature data were extracted from weather stations across Kent from the CEDA data archive (CEDA 2023). The closest weather station was matched to each orchard for monitoring data, and data were extracted (2011–2021). This also occurred for weather data used to calibrate and validate the PhenoFlex model, and data were extracted from the East Malling weather station (1959–2021). For unavailable temperature records, if gaps were short (less than 3 days) then hourly temperatures were generated using the interpolate_gaps function in chillR (Luedeling 2023), averaging temperature before and after the gap. For longer time periods, hourly temperatures were used from the closest weather station in Kent. If hourly temperatures were unavailable, then hourly temperatures were generated from daily maximum and minimum mean temperatures using the stack_hourly_temps function in the chillR package (Luedeling 2023).

For predicting temperature data for Kent, maximum and minimum daily air temperature (°C) above 1.5 m was generated from the UKCP18 (UK Climate Projections) for a 60 km by 60 km grid cell surrounding Kent (UKCP 2021). Data were generated for RCP2.6 and RCP8.5 emissions scenarios (1960–2099), based on the 15-member Hadley Centre's Perturbed Physics ensemble (PPE-15). Hourly temperatures were generated from daily maximum and minimum mean temperatures using the stack_hourly_temps function in the chillR package (Luedeling 2023). The RCP2.6 and RCP8.5 scenarios were chosen as Schwalm et al. (2020) speculates that the RCP8.5 scenario is the optimal scenario at tracking CO_2 emissions until 2050, and even by 2100, RCP8.5 is still feasible, whilst the RCP2.6 scenario contrasts strongly with this.

Data analyses

Flowering phenology

The chillR package was used to predict current and future flowering phenology for first, full and last flowering times for cv. Conference pear (Luedeling 2023), using the PhenoFlex model (Luedeling 2024; Luedeling et al. 2021). This model looks at chilling (minimum exposure period to cold

temperatures required for a tree to blossom) and forcing/heating (minimum exposure period to warmer temperatures required for a tree to blossom) periods in order to predict fruit tree blossom date. The PhenolFlex model uses the Dynamic model to calculate chill requirements (Fishman et al. 1987) and the Growing Degree Hours (GDH) model for forcing/heating requirements (Anderson et al. 1985), and requires hourly air temperature. For model calibration and validation, the data were divided into two subsets, with approximately 75% of the data for model calibration (46 years) and 25% of the data for model validation (16 years), as demonstrated in Wyver et al. (2024). A generalised simulated annealing (GenSA) algorithm was then used to optimise the parameters within the PhenoFlex model and minimise the residual sum of squares (RSS) (Tsallis and Stariolo 1996; Xiang et al. 2013). Up to 1000 iterations of this algorithm were run, stopping when there was no additional improvement in model fit after 250 consecutive iterations, as demonstrated in Wyver et al. (2024). Initial parameters were based on those established in other PhenoFlex studies (Fernandez et al. 2022; Wyver et al. 2024). To evaluate model performance, the root mean square error (RMSE) and ratio of performance to interquartile (RPIQ) distance were calculated. The parameter optimisation process was run multiple times, with staring parameters changed to that of the previous optimisation. This process was stopped after there was no improvement found to RMSE or RPIQ. Standard errors of optimum parameters were calculated using bootstrapping, using 10 iterations (Fernandez et al. 2022; Luedeling et al. 2021; Wyver et al. 2024).

Pear psyllid phenology

Pear psyllid phenology was predicted using the model by Schaub et al. (2005) and R code generated by Belien et al. (2017). This model relies on a time distributed delay and uses hourly temperatures with a microclimate correction to predict egg, nymph and adult percentage abundance for the first two generations of pear psyllid, with a start date of 01 January. The termination of diapause in psyllid females was based on a Weibull distribution and was dependent on the time spent above the thermal threshold (3.5 °C) (Schaub et al. 2005). For females where diapause was terminated, oviposition began, and summerform females had a pre-oviposition period of 10 days. Oviposition was age-specific, and the cumulative oviposition density was 1. Both egg and nymph developmental rates and adult ageing were linearly dependent on temperature based on slopes and thresholds stated within Schaub et al. (2005). A microclimate correction was used, as demonstrated in Schaub et al. (2005). For model calibration, predicted and observed peak egg, nymph and adult pear psyllid abundance (first and second generations) were compared using a nonparametric Kruskal–Wallis test. If differences between observed and predicted were significant, then abundances were shifted based on average peak difference. Future temperatures predicted under RCP2.6 and RCP8.5 scenarios were then used to predict psyllid percentage abundance from 1960 to 2080 based on calibrated models. Predicted values were generated for each orchard in comparison with observed values (between 2011 and 2021). Predicted values were also generated for the whole of Kent between 1960 and 2080, using UKCP18 data.

Earwig phenology

Earwig phenology was predicted using the degree day model developed by Moerkens et al. (2011), which was developed into a management tool (Belien et al. 2012, 2013). The degree day model predicts the first and peak appearance dates of *F. auricularia* life stages and variation in development time of earwig life stages in trees (Moerkens et al. 2011), with a start date of 01 January. Degree days were summed between the minimum and maximum developmental temperature threshold, until the minimum number of day degrees was reached for each life stage. For this model, day degrees between T_0 and T_{max} were calculated using a sine wave method. Variation in development time was modelled using a using a two-parameter Weibull function, due to environmental and individual variation within the population. A daytime microclimate correction is not present within this model as *F. auricularia* are nocturnal foragers (Kölliker 2007; Suckling et al. 2006), often found sheltering in dark crevices during the daytime (Lame 1974), and thus are not generally impacted by daytime tree microclimate (Moerkens et al. 2011).

For model calibration, predicted and observed peak stage 4 nymph abundance dates and peak adult abundance dates, for single brood populations, were compared using a Kruskal–Wallis test. Only these stages were compared, as they are both arboreal stages that agronomists were likely to observe in orchard trees and predate on pear psylla (Gobin et al. 2008; Moerkens et al. 2011). If differences between observed and predicted were significant, then abundances were shifted based on average peak difference, based on Kruskal–Wallis tests between predicted and observed values. Observed data spanned from 2011 to 2021. Future temperatures predicted under RCP2.6 and RCP8.5 scenarios were used to predict earwig percentage abundance from 1960 to 2080 based on calibrated models.

Future climate scenarios and phenological mismatches

This study tested for shifts in timing of phenological events, including: flowering time (first, full and last), pear psyllid phenology (peak egg and nymph and adult abundance)

and earwig phenology (peak stage 4 and adult emergence) depending on year (1960–2080). First, years were split into 3 different categories: historical (1960–1982), current (1983–2021) and future (2022–2080, for RCP2.6 and RCP8.5 scenarios). Timing of events were predicted using maximum and minimum temperatures generated from UKCP18 (UK Climate Projections) for a 60 km by 60 km grid cell surrounding Kent (UKCP 2021), using the three models. The change in timing of phenological event depending on year was tested using generalised additive models (GAMs); however, if the GAM had an edf < 2 and did not show a nonlinear relationship then a GLM was fitted, as used in Wyver et al. (2023). To identify phenological mismatches, the slopes of two phenological events were compared based on GAMs or GLMs generated. Phenological comparisons included: (1) first *C. pyri* nymph emergence and first flowering time, (2) peak first-generation (G1) *C. pyri* nymph abundance and full flowering time, and (3) peak second-generation (G2) *C. pyri* nymph abundance and 4th instar *F. auricularia* peak abundance. These phenological mismatches were chosen as they are relevant interactions between trophic levels within the agroecosystem. For example, G1 *C. pyri* nymphs shelter in flower buds, whilst 4th instar *F. auricularia* nymphs are a key predator of *C. pyri* nymphs during the summer; thus, these trophic levels are likely to interact. Phenological mismatches between each of these events were also calculated; this was calculated by subtracting the date (Julian days) of one phenological event from another, as demonstrated in Wyver et al. (2023). A GAM or GLM of the mismatch depending on year was plotted.

Results

Flowering phenology calibration and validation

From parameters optimised by the GenSA algorithm, the average chilling requirement was 35.97 ± 0.18 chill units for first flowering time, 47.69 ± 1.48 for full flowering and 41.56 ± 0.27 for last flowering, whilst the average forcing/heating requirement was 237.67 ± 0.56 heat units for first flowering, 287.11 ± 4.57 for full flowering and 227.88 ± 0.58 for last flowering (Table 1). Model quality was assessed by RMSE and RPIQ for calibration and validation datasets (Fig. 1). On average, the observed flowering time was 12 Apr ± 10.91 (first), 18 Apr ± 10.39 (full) and 30 Apr ± 9.75 (last), whilst the predicted flowering time was 12 Apr ± 11.96 (first), 19 Apr ± 11.72 (full) and 29 Apr ± 10.44 (last, Table 2). Kruskal–Wallis tests showed non-significant differences between predicted and observed values for first ($\chi^2 = 0.0150$, $df = 1$, $p = 0.903$), full ($\chi^2 = 0.0637$, $df = 1$, $p = 0.801$) and last ($\chi^2 = 0.0529$, $df = 1$, $p = 0.818$) flowering phenology. Chill tended to accumulate between October and January, whilst heat accumulation was between January and April, before the y_c *and* z_c thresholds were reached (Fig. 2). For temperature response curves, optimal chill accumulation was between 1 °C and 7.5 °C (Figure S2), with no chill accumulation occurring above 11 °C, whilst optimal heat accumulation was between 26 and 28 °C, with no heat accumulation occurring above 37 °C.

Pear psyllid model validation

The peak abundance of G1 psylla nymphs was predicted to be earlier than those observed within orchards (Table 2, Fig. 3A); on average, predicted peak date was 14.36 ± 17.86 (SD) days earlier than observed values in orchards. A Kruskal–Wallis test showed a significant difference between observed and expected values ($\chi^2 = 33.84$, $df = 1$, $p < 0.001$); however, the difference between individual orchards was non-significant ($\chi^2 = 15.70$, $df = 17$, $p = 0.546$). The model was therefore adjusted for G1 egg and nymph abundances, shifting them both 14.36 days later. The peak abundance of eggs was not compared, as orchards started monitoring after the abundance of eggs had peaked; thus, egg abundance peak was also shifted by 14 days.

Conversely, the peak abundance of summerform adults was similar for predicted and observed values (Table 2, Fig. 3B). On average, the predicted peak date was 2.34 ± 9.74 (SD) days later than observed values in orchards, but this was not significant (Kruskal–Wallis: $\chi^2 = 1.903$, $df = 1$, $p = 0.168$). The difference between individual orchards was also non-significant (Kruskal–Wallis: $\chi^2 = 13.75$, $df = 17$, $p = 0.685$). The peak abundance of generation 2 eggs was also closer for predicted and observed values (Table 2, Fig. 3C). The mean predicted peak date was 0.63 ± 17.11 (SD) days earlier than observed values in orchards which was not significant (Kruskal–Wallis: $\chi^2 = 0.121$, $df = 1$, $p = 0.728$), and the difference between individual orchards was also non-significant (Kruskal–Wallis: $\chi^2 = 14.64$, $df = 17$, $p = 0.745$). Finally, the peak abundance of generation 2 nymphs was close for predicted and observed values (Table 2, Fig. 3D). On average, the predicted peak date was 0.42 ± 12.74 (SD) days later than observed values in orchards (Kruskal–Wallis: $\chi^2 = 0.924$, $df = 1$, $p = 0.336$), and the difference between orchards was also non-significant ($\chi^2 = 20.86$, $df = 17$, $p = 0.233$). Summerform adult, G2 egg or G2 nymph values were not shifted within the model.

Earwig model validation

The predicted and observed dates of peak *F. auricularia* stage 4 nymph abundance did not significantly differ from each other (Kruskal–Wallis: $\chi^2 = 1.15$, $df = 1$, $p = 0.284$, Table 2, Fig. 3E). On average, the predicted date for peak

Table 1 Parameters used within the PhenoFlex model, including the initial start values and upper and lower bounds used for calibration

Parameters	Description	Initial value (lower, upper)	Optimal parameters for flowering stage		
			First	Full	Last
y_c	Chill requirement (defines the end of the chilling period)	40 (20, 80)	35.97 ± 0.18	47.69 ± 1.48	41.56 ± 0.27
z_c	Heat requirement (defines the end of the forcing period)	190 (100, 500)	237.67 ± 0.56	287.11 ± 4.57	227.88 ± 0.58
s_1	Slope parameter, defining the transition between chilling and forcing periods	0.5 (0.1, 1.0)	0.989 ± 0.231	0.211 ± 0.233	0.29 ± 0.18
T_u (°C)	Optimal temperature for the GDH model	25 (0, 30)	28.04 ± 0.00	26.73 ± 0.320	28.53 ± 0.00
E_0 (K)	Activation energy required to form the precursor to the dormancy-breaking factor (PDBF) within the Dynamic model	3372.8 (3000.0, 4000.0)	3373.12 ± 0.00	3324.80 ± 0.00	3371.86 ± 0.00
E_1 (K)	Activation energy required to destroy the precursor to the dormancy-breaking factor (PDBF) within the Dynamic model	9900.3 (9000.0, 10,000.0)	9898.92 ± 0.32	9853.98 ± 0.439	9901.74 ± 0.33
A_0 (h^{-1})	Amplitude for compound formation of PDBF within the Dynamic model	6319.5 (6000.0, 7000.0)	6090.75 ± 20.41	6218.27 ± 66.87	6008.99 ± 0.036
A_1 (h^{-1})	Amplitude for compound destruction of PDBF within the Dynamic model	5.939917e13 (5e13, 6e13)	5.939915e13 ± 6.12 e07	5.939902e13 ± 9.56 e07	5.939898e13 ± 1.34 e08
T_f (°C)	Transition temperature of the sigmoidal function within the Dynamic model	4 (0, 10)	4.56 ± 0.58	0.0589 ± 2.11	0.507 ± 1.08
T_c (°C)	Upper temperature threshold for the GDH model	36 (0, 40)	38.58 ± 1.88	27.24 ± 3.50	32.55 ± 4.05
T_b (°C)	Base temperature for the GDH model	4 (0, 10)	0.691 ± 0.022	1.21 ± 0.00	2.72 ± 0.02
s (K^{-1})	Sigmoidal function slope within the Dynamic model producing Chill Portions	1.60 (0.05, 50.00)	1.79 ± 2.56	22.00 ± 15.12	8.92 ± 11.26

As well as the optimal parameters for each flowering stage (first, full and last) for cv. Conference pear trees (*Pyrus communis*) after bootstrapping

4th instar emergence was the 21 Jun ± 7.39 (SD) whilst the observed date was the 18 Jun ± 17.09 (SD). This was also true for peak adult emergence (Table 2, Fig. 3F); predicted and observed values did not differ significantly from each other (Kruskal–Wallis: $\chi^2 = 2.06$, $df = 1$, $p = 0.151$). On average, the predicted date for peak adult emergence was 17 Aug ± 7.33 (SD), whilst the average observed value was 15 Aug ± 16.43 (SD). Observed peak dates did not significantly differ from each other depending on orchard, for both 4th instar (Kruskal–Wallis: $\chi^2 = 15.87$, $df = 17$, $p = 0.666$) and adult *F. auricularia* (Kruskal–Wallis: $\chi^2 = 8.67$, $df = 17$, $p = 0.926$). Due to the non-significant differences, the model was not shifted for *F. auricularia*.

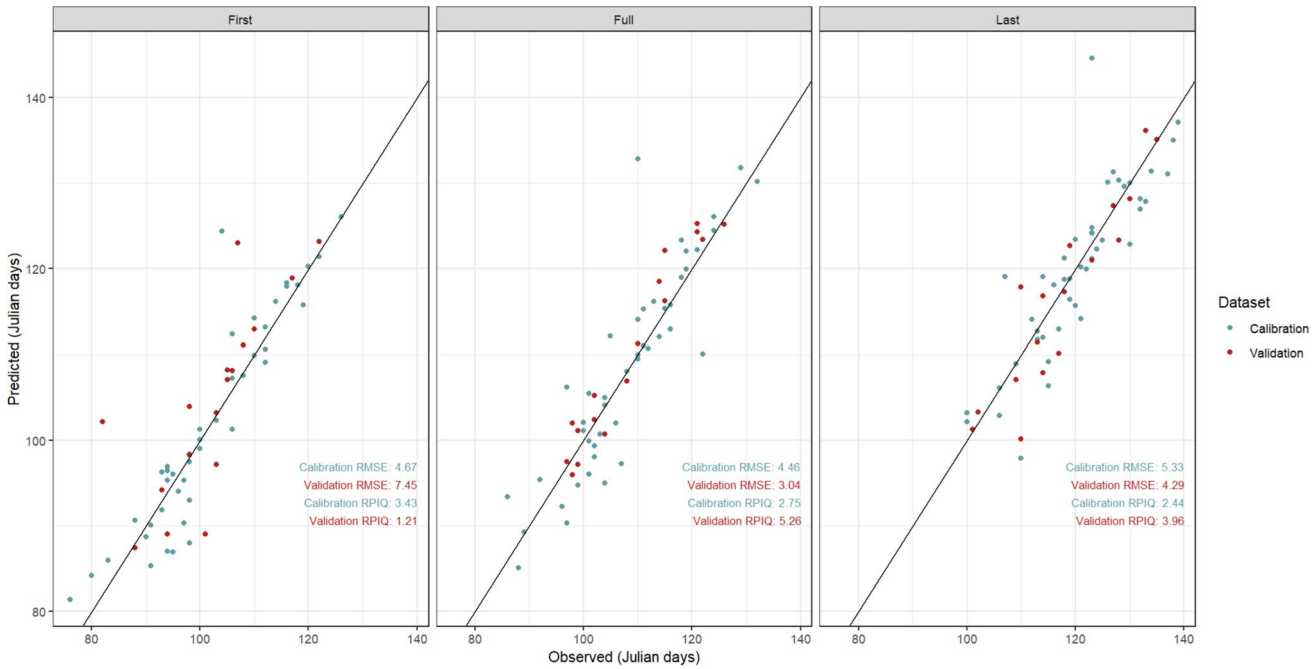

Fig. 1 Observed and predicted flowering dates (Julian days) from calibration and validation datasets, generated from the PhenoFlex model, for first, full and last flowering stages for cv. Conference pear trees (*Pyrus communis*). With the root mean square error (RMSE) and ratio of performance to interquartile (RPIQ) distance for predicted and observed values

Table 2 Average predicted and observed (data collected from orchards) peak abundance dates and difference between predicted and observed values, for cv. Conference pear (*Pyrus communis*) flowering time (first, full and last), peak abundance of *Cacopsylla pyri* eggs, nymphs and adults and peak abundance of *Forficula auricularia* arboreal nymphs and adults

Phenological stage	Species	Predicted peak date	Observed peak date	Difference (days)	*P* value	RMSE
First flowering	*Pyrus communis*	12 Apr ± 1.24	12 Apr ± 1.52	0.57 ± 0.71	0.903	4.67
Full flowering	*Pyrus communis*	19 Apr ± 1.32	18 Apr ± 1.49	0.57 ± 0.63	0.801	4.46
Last flowering	*Pyrus communis*	29 Apr ± 1.23	30 Apr ± 1.33	− 0.62 ± 0.64	0.818	5.33
G1 nymphs	*Cacopsylla pyri*	24 Apr ± 1.13	09 May ± 1.95	− 14.36 ± 1.94	**< 0.001**	**22.84**
Summerform adults	*Cacopsylla pyri*	25 May ± 0.80	23 May ± 1.13	2.34 ± 1.06	0.168	9.97
G2 eggs	*Cacopsylla pyri*	02 Jun ± 0.83	02 Jun ± 1.88	− 0.63 ± 1.84	0.728	17.03
G2 nymphs	*Cacopsylla pyri*	25 Jun ± 0.77	25 Jun ± 1.38	0.42 ± 1.38	0.336	12.68
4th instar nymphs	*Forficula auricularia*	21 Jun ± 0.85	18 Jun ± 1.96	2.54 ± 2.12	0.284	18.56
Adults	*Forficula auricularia*	17 Aug ± 0.92	15 Aug ± 2.05	2.68 ± 1.81	0.151	14.61

P values in bold show significant differences between predicted and observed values based on Kruskal–Wallis tests. The RMSE (root mean square error) of model prediction is also presented

Climate predictions and phenological shifts

All flowering stages (first, full and last) showed significant advancement in flowering time depending on year, becoming significantly earlier between 1983 and 2021 (Table 3). However, this advancement was not significant for the historical time period (1960–1982), suggesting the advancement began in the 1980s. Based on the PhenoFlex model, average first flowering time was predicted to advance from the 04 May ± 4.66 SD (1960–1983) to 19 Apr ± 4.63 SD (2011–2021), becoming 15 days earlier, whilst full flowering time shifted from 13 May ± 3.99 SD (1960–1983) to 29 Apr ± 4.05 SD (2011–2021), a 14-day advancement. This shift was predicted to continue under future emissions scenarios, a GLM predicted earlier first flowering time depending on year (2022–2080, Table 4), at a rate of − 0.177 days per year under the RCP8.5 (high) emissions scenario. On average, the first flowering date was predicted to be 07 Apr ± 2.69 SD between 2060 and 2080, under RCP8.5. However, this was non-significant for the RCP2.6 scenario (Table 4). For full flowering time, flowering phenology advanced significantly under RCP2.6 and RCP8.5 emissions

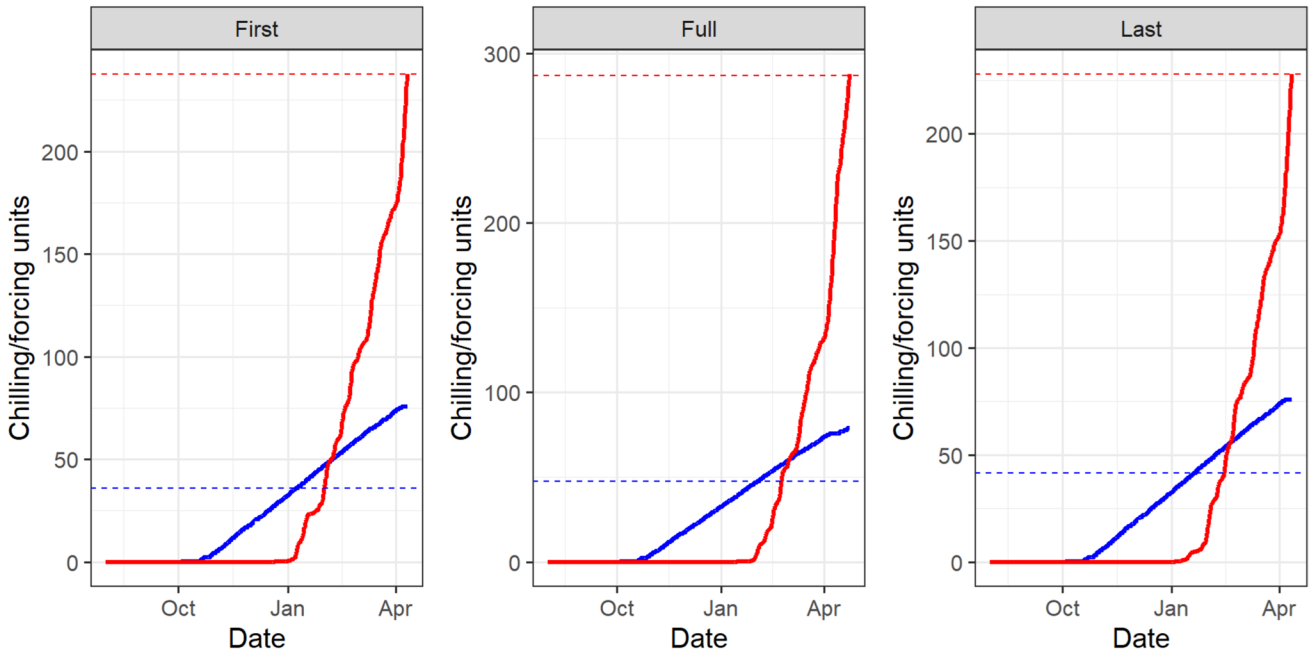

Fig. 2 Chill and heat accumulation curves for cv. Conference pear trees (*Pyrus communis*), for first, full and last flowering phenology, during 2021. The blue solid line represents chill accumulation and the red solid line represents heat accumulation. The blue dashed line represents yc (the threshold for end of chill accumulation) and the red dashed line represents zc (the threshold for end of heat accumulation)

scenarios, at a rate of −0.053 days and −0.197 days per year, with an average full flowering date predicted as 20 Apr ± 2.21 SD (RCP2.6) and 16 Apr ± 2.31 SD (RCP8.5).

Cacopsylla pyri phenology peak G1 nymph abundance changed significantly depending on year (1983–2021). Once again, this change was non-significant for the historical time period (1960–1982). The mean peak G1 nymph abundance date was 25 May ± 8.37 SD (1960–1982) and 11 May ± 14.52 (2011–2021). This phenological shift was predicted to continue under future emissions scenarios, a GLM predicted earlier G1 peak *C. pyri* nymph abundance depending on year (2022–2080, Table 3), at a rate of −0.413 days per year (RCP8.5 scenario). On average, the G1 peak nymph abundance date was predicted to be 16 Apr ± 11.37 SD between 2060 and 2080, under RCP8.5. However, this was non-significant for the RCP2.6 scenario (Table 3, Fig. 4). For first G1 peak *C. pyri* nymph emergence, phenology did not significantly change depending on year for historic, current or RCP2.6 emissions scenarios. Only under the RCP8.5 scenario did emergence times become significantly earlier (Figure S4), at a rate of −0.125 days per year (Fig. 5). For G2 *C. pyri* nymphs, peak abundance also differed significantly depending on year under the current time period, shifting at rate of −0.403 days per year (Fig. 6). The mean peak abundance date was 11 Jul ± 4.47 SD for the historical time period (1960–1982) and 26 Jun ± 11.10 SD for 2011–2021. Peak abundance for G2 nymphs was predicted to continue to shift under the RCP8.5 emissions scenario (2022–2080) at a rate of −0.315 days per year; however, this shift was non-significant for the RCP2.6 scenario (Table 3).

Forficula auricularia stage 4 nymph peak abundance date changed significantly depending on year (1983–2021), at a rate of −0.375 days per year (Table 3). The mean peak *F. auricularia* nymph abundance date was 08 Jul ± 4.59 SD (1960–1982) and 22 Jun ± 10.11 SD (2011–2021). Peak abundance for *F. auricularia* nymphs was predicted to continue to shift under the RCP8.5 scenario (2022–2080) at a rate of −0.288 days per year (Fig. 7); however, this shift was non-significant for RCP2.6 (Table 3). This was similar for the peak abundance date of *F. auricularia* adults, under the current time period peak abundance date advanced significantly, at a rate of −0.508 days per year (Table 3). Peak abundance date shifted from an average of 06 Sep ± 8.97 (1960–1982) to 12 Aug ± 10.56 (2011–2021). Peak abundance for *F. auricularia* adults was predicted to continue to shift under RCP8.5 (2022–2080) at a rate of −0.224 days per year; however, this shift was non-significant for RCP2.6 (Table 3).

Phenological differences and mismatches

The phenological difference between full flowering time and G1 peak *C. pyri* nymph abundance date was not significant depending on year for historical, current or RCP2.6 scenarios (Table 5). However, the phenological difference did significantly change at a rate of 0.216 days

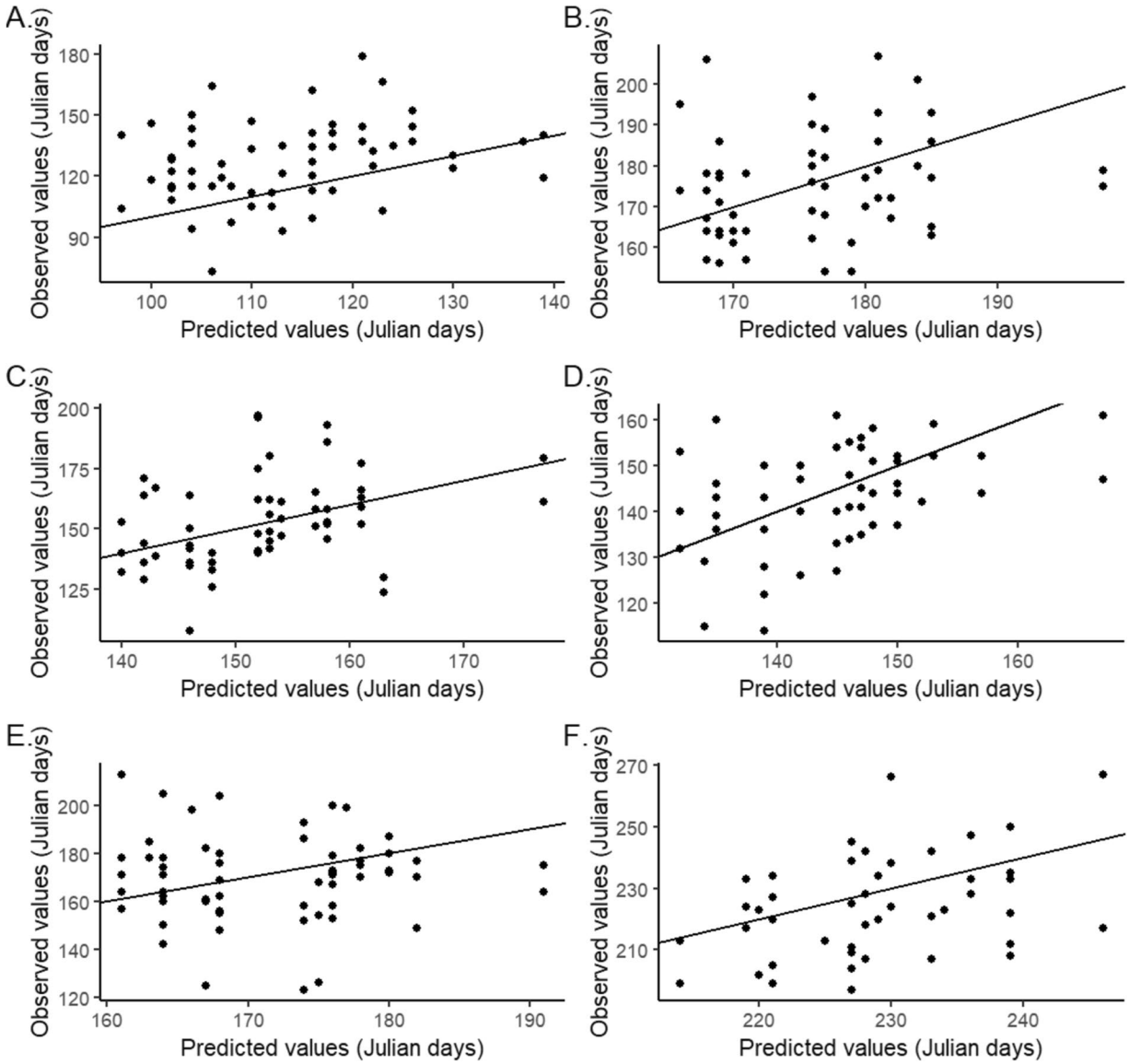

Fig. 3 Observed and predicted values (Julian days) for *Cacopsylla pyri* and *Forficula auricularia* phenological events, generated from the psyllid phenology model, for A. peak *Cacopsylla pyri* G1 peak nymph abundance, B. peak *Cacopsylla pyri* G2 peak nymph abundance, C. peak *Cacopsylla pyri* G2 peak egg abundance, D. peak *Cacopsylla pyri* peak summerform adult abundance, E. peak *Forficula auricularia* stage 4 nymph abundance and F. peak *Forficula auricularia* adult abundance. The black line has a gradient = 1, intercept = 0, to show where the points should be if predicted and observed values matched each other

per year under the RCP8.5 scenario, shifting from a mean difference of -11.74 ± 13.01 SD days (2011–2021), to 0.349 ± 12.40 SD days between the two trophic levels. The average advancement in phenology for *C. pyri* G1 peak nymph abundance is predicted to shift at a faster rate (-0.413) compared to full flowering time (-0.197) under RCP8.5. This could potentially lead to a phenological mismatch, where peak nymph abundance occurs before full flowering time after 2071 (Fig. 4). For all other phenological events, no significant relationship was found between the phenological difference and year, for all other pairs of trophic levels (Table 5). The rate of change for G2 *C. pyri* peak nymph emergence and *F. auricularia* peak stage 4 nymph abundance dates was similar (Fig. 6), under current (-0.403 and -0.375) and RCP8.5 (-0.315 and -0.288) scenarios. Furthermore, there was a large amount of overlap between *C. pyri* and *F. auricularia* nymph abundance peaks for all scenarios (Fig. 8), highlighting phenological synchrony.

Table 3 Model parameters for each phenological event and scenario, based on the relationship between event date (Julian days) and year

Stage	Scenario	Model Type	Gradient	SE	Edf	Intercept	*F* statistic	R^2 adjusted	*p*-value
First flowering *Pyrus communis*	Historical	GLM	−0.254	0.140	1.00	624.62	3.32	9.53	0.0828
	Current	GAM	~	0.621	2.81	113.90	15.61	58.50	**< 0.001**
	RCP2.6	GLM	−0.0443	0.0226	1.00	193.20	3.87	4.71	0.0540
	RCP8.5	GLM	−0.177	0.0206	1.00	464.22	74.42	55.87	**< 0.001**
Full flowering *Pyrus communis*	Historical	GLM	−0.1998	0.123	1.00	526.77	2.62	11.09	0.120
	Current	GAM	~	0.542	2.82	123.56	16.71	63.23	**< 0.001**
	RCP2.6	GLM	−0.0528	0.0197	1.00	220.17	7.18	9.63	**0.00961**
	RCP8.5	GLM	−0.197	0.0181	1.00	514.20	119.20	67.09	**< 0.001**
Last flowering *Pyrus communis*	Historical	GLM	−0.161	0.101	1.00	459.39	2.54	6.55	0.126
	Current	GAM	~	0.487	5.36	134.78	10.48	63.20	**0.0004**
	RCP2.6	GLM	−0.0657	0.0174	1.00	257.50	14.27	18.61	**< 0.001**
	RCP8.5	GLM	−0.222	0.0160	1.00	575.45	191.77	76.68	**< 0.001**
G1 *Cacopsylla pyri* first nymph emergence	Historical	GLM	−0.152	0.500	1.00	339.37	0.0925	-4.30	0.764
	Current	GLM	−0.328	0.212	1.00	696.86	2.40	3.55	0.130
	RCP2.6	GAM	~	1.36	4.30	35.41	1.12	5.43	0.408
	RCP8.5	GLM	−0.125	0.0524	1.45	287.87	5.71	7.52	**0.0202**
G1 *Cacopsylla pyri* nymph peak abundance	Historical	GLM	−0.0524	0.269	1.00	248.65	0.0379	-4.57	0.848
	Current	GAM	~	2.10	2.92	138.00	2.43	17.64	**0.0138**
	RCP2.6	GLM	0.0710	0.109	1.00	-22.44	0.422	-1.01	0.519
	RCP8.5	GLM	−0.413	0.0908	1.00	961.42	20.70	25.36	**< 0.001**
G1 *Cacopsylla pyri* summerform adults peak abundance	Historical	GLM	0.0464	0.197	1.00	70.46	0.0558	4.48	0.816
	Current	GAM	~	1.61	2.67	154.41	3.26	20.50	**0.0263**
	RCP2.6	GLM	0.0499	0.0787	1.00	39.22	0.402	1.04	0.528
	RCP8.5	GLM	−0.362	0.0754	1.00	875.78	23.12	28.85	**< 0.001**
G2 *Cacopsylla pyri* egg peak abundance	Historical	GLM	0.0652	0.190	1.00	41.02	0.118	-4.17	0.734
	Current	GLM	−0.428	0.140	1.00	1018.14	9.28	17.90	**0.004**
	RCP2.6	GLM	0.0421	0.0750	1.00	62.69	0.315	-1.20	0.577
	RCP8.5	GLM	−0.353	0.0727	1.00	865.54	23.62	28.06	**< 0.001**
G2 *Cacopsylla pyri* nymph peak abundance	Historical	GLM	−0.00988	0.144	1.00	211.56	0.00472	4.74	0.946
	Current	GLM	−0.403	0.130	1.00	990.79	9.67	18.57	**0.004**
	RCP2.6	GLM	0.0140	0.0669	1.00	142.72	0.0437	1.68	0.835
	RCP8.5	GLM	−0.315	0.0627	1.00	810.54	25.29	29.52	**< 0.001**
Forficula auricularia stage 4 peak nymph abundance	Historical	GLM	−0.0148	0.148	1.00	218.08	0.0101	-0.0471	0.921
	Current	GLM	−0.375	0.120	1.00	930.24	9.75	18.72	**0.003**
	RCP2.6	GLM	−0.00625	0.0611	1.00	181.11	0.0105	-1.74	0.919
	RCP8.5	GLM	−0.288	0.0629	1.00	752.88	20.99	25.63	**< 0.001**
Forficula auricularia peak adult abundance	Historical	GLM	−0.132	0.287	1.00	510.20	0.212	3.71	0.650
	Current	GLM	−0.508	0.138	1.00	1251.01	13.61	24.92	**0.001**
	RCP2.6	GLM	−0.025	0.0595	1.00	268.90	0.177	1.44	0.676
	RCP8.5	GLM	−0.224	0.0608	1.57	672.54	13.57	19.23	**0.001**

GLMs were fitted if the edf of the GAM was < 2, *p*-values in bold show a significant relationship

Discussion

Phenological shifts over time

Our analyses suggest that the timing of at least one phenological event has changed for each trophic level. Firstly, flowering time for first, full and last phenological stages has become earlier in the year as a result of climate change. This is supported by multiple studies, suggesting that temperature significantly influences budburst and flowering phenology (Amano et al. 2010; Auffret 2021; Fitter and Fitter 2002). Pear trees are heavily influenced by temperature, entering endodormancy during late autumn where growth is inhibited (Atkinson et al. 2013, 2004; Drepper

Table 4 Average predicted dates ± standard error for phenological events depending on scenario (historic, current, RCP2.6 and RCP8.5)

Phenological stage	Species	Historical (1960–1983)	Current (2011–2021)	RCP 2.6 (2060–2080)	RCP 8.5 (2060–2080)
First flowering	*Pyrus communis*	04 May ± 0.97	19 Apr ± 1.39	11 Apr ± 0.54	07 Apr ± 0.59
Full flowering	*Pyrus communis*	13 May ± 0.85	29 Apr ± 1.22	20 Apr ± 0.48	16 Apr ± 0.50
Last flowering	*Pyrus communis*	23 May ± 0.69	10 May ± 1.09	01 May ± 0.50	25 Apr ± 0.48
G1 nymphs (First emergence)	*Cacopsylla pyri*	08 Feb ± 3.13	07 Feb ± 3.89	07 Feb ± 2.65	28 Jan ± 0.83
G1 nymphs (Peak emergence)	*Cacopsylla pyri*	25 May ± 1.75	11 May 4.38	06 May ± 3.15	16 Apr ± 2.48
Summerform adults	*Cacopsylla pyri*	11 Jun ± 1.28	27 May ± 3.40	23 May ± 2.37	05 May ± 1.94
G2 eggs	*Cacopsylla pyri*	19 Jun ± 1.23	04 Jun ± 3.39	31 May ± 2.28	14 May ± 1.91
G2 nymphs	*Cacopsylla pyri*	11 Jul ± 0.93	26 Jun ± 3.35	21 Jun ± 2.03	08 Jun ± 1.43
4th instar nymphs	*Forficula auricularia*	08 Jul ± 0.96	22 Jun ± 3.05	18 Jun ± 1.90	06 Jun ± 1.38
Adults	*Forficula auricularia*	06 Sep ± 1.79	12 Aug ± 3.19	06 Aug ± 1.92	28 Jul ± 1.82

Events include cv. Conference pear (*Pyrus communis*) flowering time (first, full and last), peak abundance of *C. pyri* eggs, nymphs and adults and first emergence of *Cacopsylla pyri* nymphs and peak abundance of *Forficula auricularia* arboreal nymphs and adults

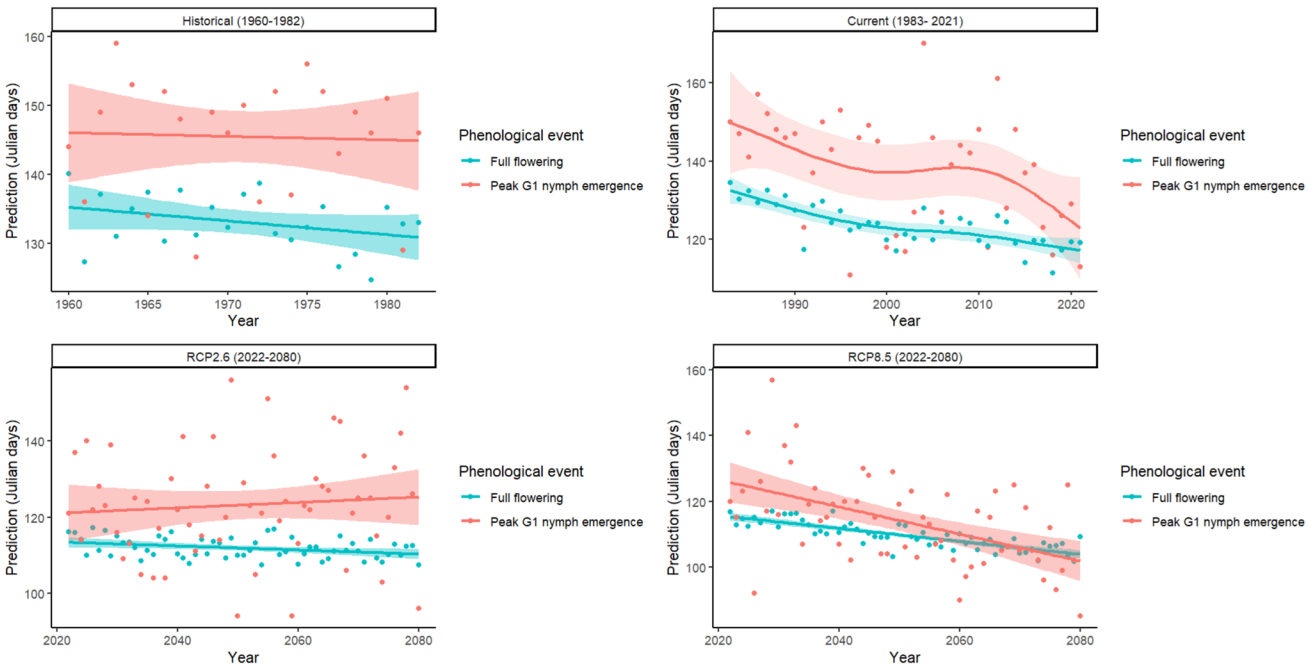

Fig. 4 Phenological shift in full flowering time (Julian days) for cv. Conference pear trees (*Pyrus communis*) and *Cacopsylla pyri* G1 peak nymph abundance date, depending on year (1960–2080) and RCP scenario (RCP2.6 and RCP8.5)

et al. 2020), until the chill requirement (hours below a certain temperature) is met. Once the chilling requirement has been reached, ecodormancy begins, where growing degree hours are accumulated; thus, elevated temperatures can lead to earlier flowering times (Drepper et al. 2020; Fadón et al. 2023). Studies have documented phenological advancements in pear flowering time depending on year and temperature (Drepper et al. 2020; Reeves et al. 2022; Sparks et al. 2005); Sparks et al. (2005) found that average first flowering time of pear had shifted to 15 Apr compared to 23 Apr for the historical time period, advancing at a rate of − 0.306 days per year.

In addition, the timing of *C. pyri* phenological events has shifted over time. G1 and G2 *C. pyri* peak nymph abundance, G2 peak egg abundance and peak summerform adult abundance, have all advanced significantly by approximately 14–15 days (current compared to historical time periods). Pear psylla are poikilothermic (Kapatos and Stratopoulou 1999; McMullen and Jong 1977), and so, elevated temperatures can have a significant impact on their metabolism,

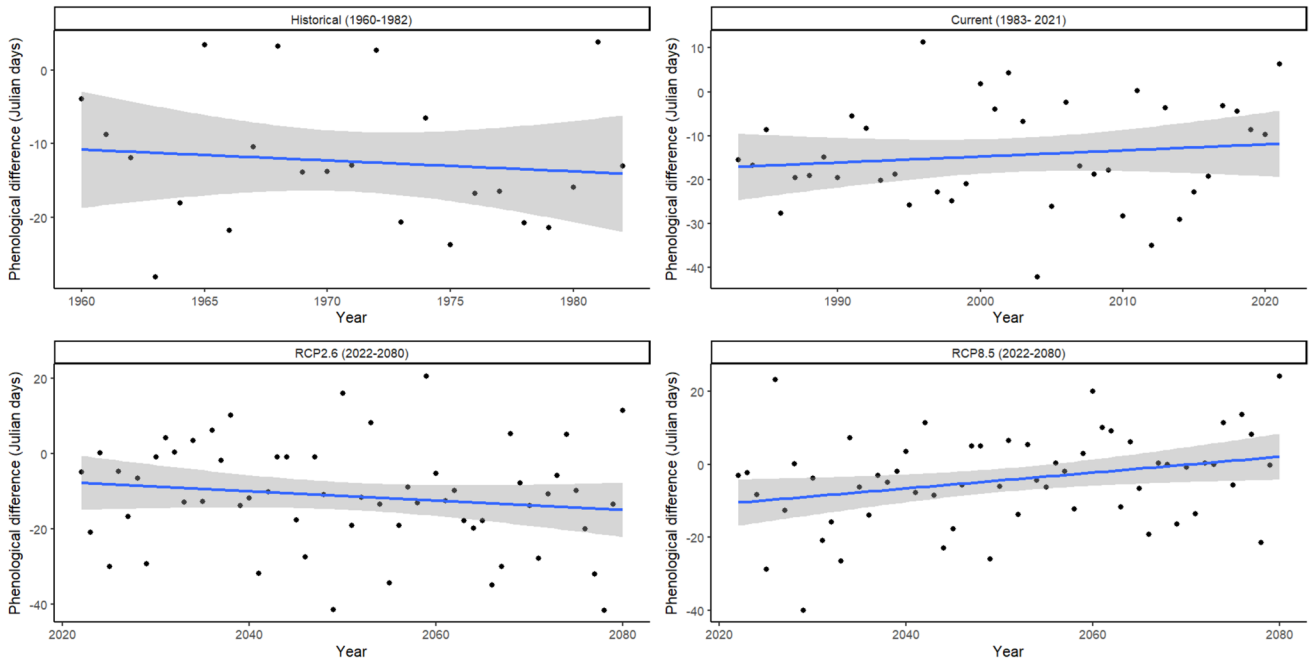

Fig. 5 Phenological difference between full flowering time (Julian days) for cv. Conference pear trees (*Pyrus communis*) and *Cacopsylla pyri* G1 peak nymph abundance date, depending on year (1960–2080) and RCP scenario (RCP2.6 and RCP8.5)

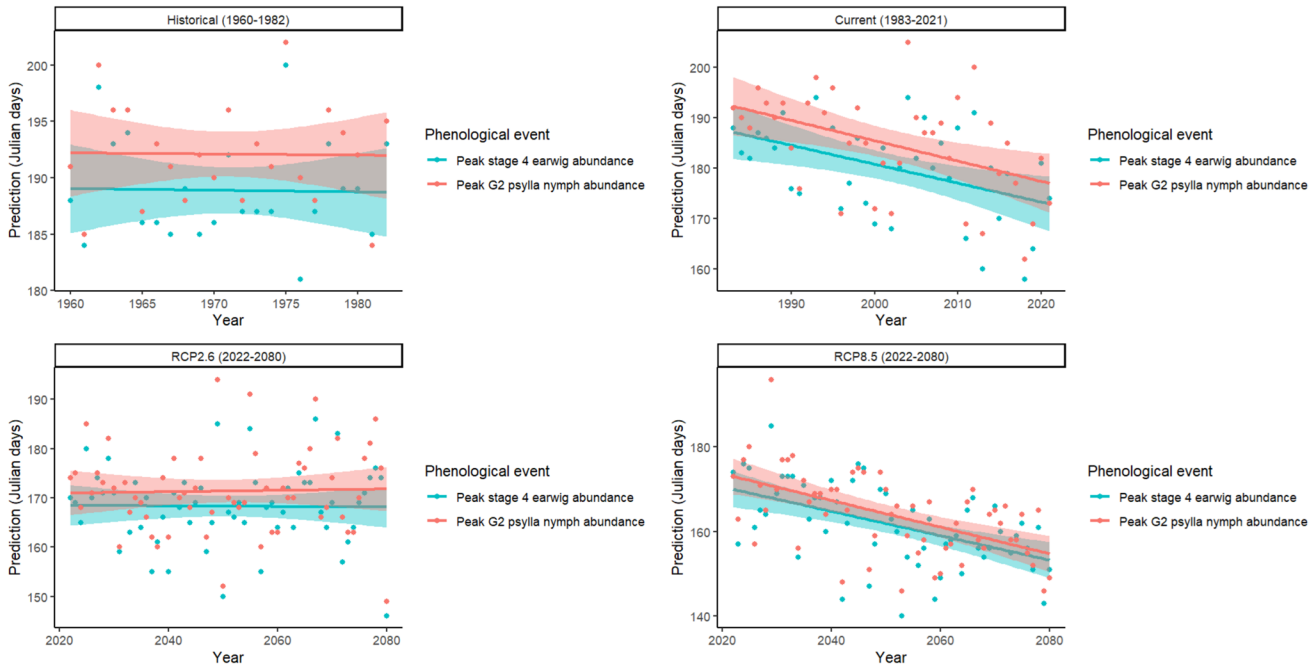

Fig. 6 Phenological shift in *Cacopsylla pyri* G2 peak nymph abundance date (Julian days) and *Forficula auricularia* stage 4 peak nymph abundance date, depending on year (1960–2080) and RCP scenario (RCP2.6 and RCP8.5)

especially in increasing the rate of enzymatically catalysed reactions (Neven 2000). McMullen and Jong (1977) found that the development rate of *C. pyricola* eggs and nymphs was significantly slower at lower temperatures; on average, taking 61.8 days to complete development at 10 °C, compared to 27.0 days at 27 °C, development rate reached a critical thermal maximum at 32.2 °C, as psyllid mortality was 100%. Earwigs are also poikilothermic (Moerkens et al.

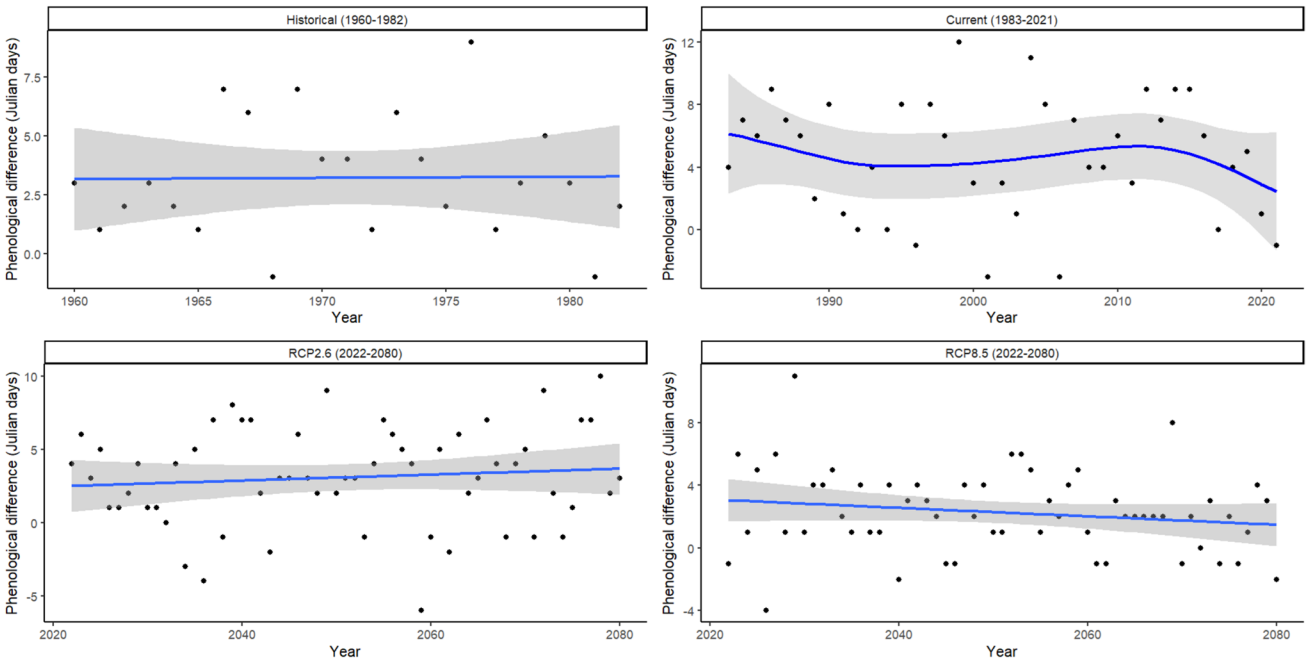

Fig. 7 Phenological difference between *Cacopsylla pyri* G2 peak nymph abundance date (Julian days) and *Forficula auricularia* stage 4 peak nymph abundance, depending on year (1960–2080) and RCP scenario (RCP2.6 and RCP8.5)

Table 5 Model parameters for the difference between two phenological events, depending on scenario, based on the relationship between phenological difference (Julian days) and year

Difference	Scenario	Model type	Gradient	SE	Edf	Intercept	*F* statistic	R^2 adjusted	*p*-value
First flowering and First *Cacopsylla pyri* nymph emergence	Historical	GLM	−0.102	0.577	1.00	285.24	0.0312	−4.61	0.862
	Current	GLM	−0.0625	0.194	1.00	198.45	0.104	−2.42	0.749
	RCP2.6	GAM	~	1.35	4.39	66.84	1.35	7.30	0.296
	RCP8.5	GLM	−0.0519	0.0566	1.58	176.35	0.841	−0.275	0.363
Full flowering and Peak *Cacopsylla pyri* G1 nymph emergence	Historical	GLM	−0.147	0.294	1.00	278.12	0.251	−3.52	0.621
	Current	GLM	0.138	0.169	1.00	−291.45	0.674	−0.866	0.417
	RCP2.6	GLM	−0.123	0.107	1.00	242.61	1.35	0.605	0.250
	RCP8.5	GLM	0.216	0.0937	1.00	−447.22	5.31	6.92	**0.0248**
Peak G2 *Cacopsylla pyri* egg abundance and Peak *Forficula auricularia* stage 4 nymph abundance	Historical	GLM	0.0800	0.145	1.00	−177.06	0.305	−3.26	0.587
	Current	GAM	–	0.832	3.06	−18.28	1.03	7.69	0.344
	RCP2.6	GLM	0.0483	0.0389	1.00	−118.42	1.54	2.64	0.219
	RCP8.5	GLM	−0.0652	0.0365	1.00	112.66	3.20	3.65	0.0790
Peak G2 *Cacopsylla pyri* nymph emergence and Peak *Forficula auricularia* stage 4 nymph abundance	Historical	GLM	0.00494	0.0823	1.64	−6.52	0.00361	−4.74	0.953
	Current	GAM	~	0.600	3.03	4.615	0.543	2.87	0.626
	RCP2.6	GLM	0.0202	0.0261	1.00	−38.39	0.603	−0.690	0.441
	RCP8.5	GLM	−0.0270	0.0202	1.00	57.65	1.79	1.34	0.186

GLMs were fitted if the edf of the GAM was < 2, *p*-values in bold show a significant relationship

2011), and development is highly temperature dependent (Belien et al. 2012; Helsen et al. 1998; Moerkens et al. 2011). Similar to *C. pyri*, *F. auricularia* peak abundance dates have advanced, with stage 4 nymphs becoming 16 days earlier and adults becoming 25 days earlier (current compared to historical predictions).

Phenological synchrony and mismatches

Based on the analyses from this study, G1 and G2 peak *C. pyri* nymph emergence date, first, full and last flowering times and *F. auricularia* stage 4 nymph and adult peak emergence date were all predicted to advance (2022–2080),

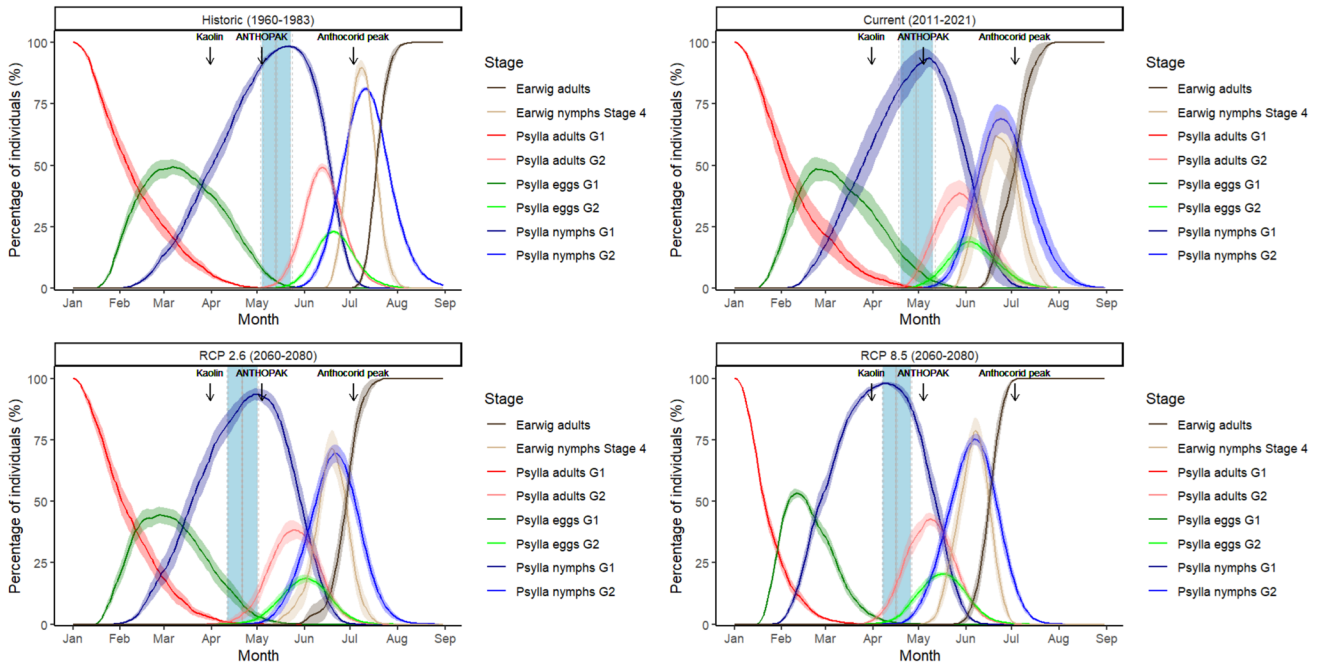

Fig. 8 Average percentage abundance of *Cacopsylla pyri*: G1 adults (red), G1 eggs (green), G1 nymphs (blue), G2 adults (orange), G2 eggs (purple), G2 nymphs (pink) and *Forficula auricularia* stage 4 nymphs (light brown) and adults (dark brown) depending on month, for each scenario. The light blue rectangle represents the flowering spread of *Pyrus communis* (from first flowering to last flowering), solid grey line the average full flowering time and dotted grey lines the standard errors. Black arrows represent key times for spray application or biological control including average Kaolin application time, average ANTHOPAK application (artificial mass release of anthocorid adults) and average anthocorid peak within orchards

under the RCP8.5 scenario. Phenological shifts have been predicted for multiple pest species under future temperature scenarios (Ju et al. 2017; Lee et al. 2016; Stoeckli et al. 2012). One study by Stoeckli et al. (2012) looked at peak larval emergence for G1 and G2 of the Lepidoptera orchard pest, codling moth (*Cydia pomonella*) under current and predicted future climate scenarios (2045–2074). Findings indicated a significant two-week advancement, for multiple phenological events including adult flight date, oviposition and larval emergence, supporting our predictions in phenological shifts. There was a significant increase in risk of a third generation of *C. pomonella*, as Switzerland currently only experiences two generations. This increase in voltinism is pertinent, as the number of generations of *C. pyri* per year is also climate dependent (Kapatos and Stratopoulou 1999; Reeves et al. 2024), with an average of 3–5 generations per year in the UK (Reeves et al. 2024). However, warmer climates such as Greece *C. pyri* produce 5–6 generations (Stratopoulou and Kapatos 1992), whilst cooler climates such as Norway produce 2 generations (Næss 2016). Therefore, a psyllid phenology model that considers generations throughout the year would be ideal, to allow researchers to consider voltinism.

There are concerns that not all trophic levels are advancing at the same rate, which can result in trophic mismatches and increased challenges for pest management (Harrington et al. 1999; Reeves et al. 2024; Renner and Zohner 2018; Wyver et al. 2023). One significant phenological difference within our study was between full flowering time and G1 *C. pyri* peak nymph abundance date; on average, full flowering time was significantly earlier than peak G1 *C. pyri* nymph abundance for current and historical scenarios. Under the RCP8.5 scenario, peak flowering time and nymph emergence began to overlap, and by 2071, peak nymph emergence date becomes earlier than full flowering time. Availability of open flower buds may be important to *C. pyri*; nymphs often shelter inside them (Solomon et al. 1989), providing protection from harsh weather conditions, agrochemical sprays and natural enemies (Reeves et al. 2022, 2024). This may be especially beneficial for younger softshell nymphs earlier in the season (L1–L3), which are smaller and more vulnerable. Thus, phenological synchrony between *C. pyri* nymphs and full flowering time may be sub-optimal for growers. Instead, nymph emergence that peaks before budburst may be more manageable when applying crop protection products. This is relevant for the application of kaolin, a non-toxic clay particle film that can be sprayed onto plant surfaces, creating a barrier that can deter oviposition and reduced movement of *C. pyri* (Erler and Cetin 2007; Saour et al. 2010). Pasqualini et al. 2002 initially investigated kaolin spray; kaolin was

applied before the onset of egg laying during overwintering. There was a 99% reduction in nymphs and eggs, during March and April compared to untreated control trees. Coverage of this spray is improved when it is applied pre-bloom (February to early April), as there is less foliage (DuPont et al. 2021; Nottingham and Beers 2020). Currently average kaolin application for the 18 orchards assessed was 30 March, which is still within the pre-bloom stage under the future RCP8.5 emissions scenario.

No significant differences between any other key trophic interactions were detected. This may be beneficial for pear growers, as the interaction between G2 *C. pyri* nymphs and earwigs remained unchanged. In historical and current scenarios, the phenological difference between peak G2 *C. pyri* nymph abundance and peak stage 4 earwig abundance dates was small, suggesting phenological synchrony. This phenological difference did not significantly change under future climate scenarios; under the RCP 8.5 scenario, the average difference was 2 days. However, there is still the question of how other natural enemies will react to rising temperatures, especially the key biological control agent *A. nemoralis*. Anthocorids show temperature-dependent development (Bonte et al. 2012; Martínez-García et al. 2018; Yanik and Unlu 2011); a study by Yanik and Unlu (2011) found that *Anthocoris minki* nymphs took 18.6 days to develop under 20 °C and 11.8 days under 30 °C. A study by Civolani and Pasqualini 2003 has evaluated the population dynamics of *A. nemoralis* with respect to *C. pyri*, in pear orchards in Italy during September–December. However, degree day models are yet to be developed for *A. nemoralis*. Based on the 18 orchards assessed, on average *A. nemoralis* were released on 04 May and adult populations peaked 04 July. Therefore, whether this biocontrol agent needs to be released earlier in the year requires future research.

Model evaluation

Observed and predicted results did not significantly differ from each other for the PhenoFlex model, *C. pyri* phenology model and *F. auricularia* degree day model, with the exception of G1 *C. pyri* peak nymph abundance date, which was on average 14 days later than predicted. There may multiple reasons for the difference between the predicted and observed values; firstly, the pear psyllid phenology model was originally optimised based on data from Switzerland (Schaub et al. 2005), potentially differing compared to UK climate. The accuracy of the weather station itself could explain the difference; most orchards were a few miles away from their corresponding weather stations; thus, temperatures experienced in orchards may not be exact. Moreover, the pear psyllid model is sensitive to small systematic errors; for example, a change of 1, 2 °C produced simulations that were 5 or 10 days earlier in Schaub et al. (2005), this could be more apparent in March–May when temperatures are more variable. Therefore, this study recommends the collection of temperature data within orchards alongside phenological monitoring data.

Data from this study were collected weekly, so perhaps more regular sampling is required, as phenological peaks can be easily missed. Furthermore, pear psyllid nymphs are more visible when shoot growth has started after flowering; before flowering, nymphs often hide in the buds or bud scales and L1–L3 nymphs are much smaller (Chang 1977). It may be more difficult for growers to observe smaller instars earlier in the season, especially using a hand lens. To help mitigate this bias of 'hidden nymphs', the 'wash down' method is recommended: washing-down foliage and budwood using water containing 1% detergent, then straining through filter paper to concentrate the nymphs and using a binocular dissecting microscope for counts (Jenser et al. 2010). This could be used to evaluate bias, but it is more labour-intensive and requires specialist equipment. Finally, the heterogeneity of the landscape could explain the later nymph peak; adult psyllids often disperse over the winter away from the host plant; however, the proportion of an orchard's population that overwinters in the orchard rather than dispersing is not known and appears to vary between years and regions (Horton 1999). One theory is that large pear monocultures see lower rates of dispersal, and thus may have earlier peaks for egg laying and G1 nymph abundance. However, the orchards used within our study were surrounded by a heterogenous landscape compared to those used in Schaub et al. (2005); therefore, more time may be required for re-entry into the orchard, resulting in later peaks.

For the earwig degree day model, a previous study found significant differences between observed and predicted emergence dates, for all life stages within apple orchards in Spain (Lordan et al. 2015); on average, peak abundance date was predicted as 29 Apr for stage 4 *F. auricularia* nymphs, but observed date was 13 May. Thus, this model may be sub-optimal for Mediterranean orchards. However, for UK orchards, observed and predicted dates for *F. auricularia* stage 4 nymphs and adults did not differ significantly. Therefore, the use of this model within UK pear orchards may be effective at predicting emergence dates; however, egg hatching and stage 1–3 peak abundance dates need to be evaluated. Another limitation within the study is the temperature data used within the *F. auricularia* degree day model. Moerkens et al. (2011) recommend the use of soil temperature (5–10 cm below the soil surface) to predict development and emergence for earlier egg and nymph stages (egg, L1 and L2); however, hourly soil temperature was not available between 2011 and 2021 for the majority of weather stations in Kent or for UKCP18 temperature predictions. This is especially important for double-brood populations due to a higher proportion of time spent within the soil throughout

the year (due to two broods in the soil a year); therefore, the collection of hourly soil temperature is recommended.

It should also be noted that the earwig degree day model and *C. pyri* phenology model are independent of each other. However, it is likely models would interact, as *F. auricularia*, can significantly reduce pear psyllid populations, although earwigs are unlikely to migrate into orchards based on psyllid density (Lenfant et al. 1994). Thus, a time distributed delay model that considers predator–prey interactions, such as those seen in the stagePop package in R may be beneficial to growers, alongside phenological models for other natural enemy species such as *A. nemoralis*, as this may alter decisions on agrochemical sprays or the further release of biological control agents. In addition, the model did not take into account management methods within the orchard or the size of the orchard, which have the potential to impact phenology. For example, tree shape, and pruning intensity and timing can affect canopy microclimate (Van den Dool 2006; Sansavini and Musacchi 2000), which can impact pest and natural enemy development times. Thus, with a larger sample size with a range of different orchard sizes and management practises these differences could be accounted for in future models.

Conclusion

To conclude the PhenoFlex model, *C. pyri* phenology model and *F. auricularia* degree day model were reasonably accurate in predicting key phenological events in UK pear orchards. Observed and predicted results did not significantly differ from each other, with the exception of G1 *C. pyri* peak nymph abundance date. All phenological events were predicted to advance under the RCP8.5 scenario, but only pear flowering time (full and last) was predicted to significantly advance under the RCP2.6 scenario. However, there was only a significant change in phenological difference between *C. pyri* peak G1 nymph abundance and full flowering time, as nymph abundance date was advancing at a faster rate. The phenological synchrony between stage 4 earwig nymphs and *C. pyri* G2 nymphs was evident in all scenarios, due to a minimal phenological difference that did not significantly change over time. However, the pear psyllid phenology model only included the first two generations, so we could not assess mismatches later in the year. In addition, a degree day model has not been developed for *A. nemoralis*, which is a key biological control agent for *C. pyri*. This study is relevant within the field of integrated pest management, linking models of crops, pests and natural enemies to better predict trophic interactions and optimise timing of management methods with respect to peak abundance dates. The PhenoFlex model can be easily optimised to multiple tree fruit crops, whilst phenological degree day models can be adapted to other pest and natural enemy development times. Thus, we recommend the long-term collection of phenological monitoring data for multiple agroecosystems, to help validate and develop a range of phenological models for key crop, pest and natural enemy species.

Supplementary Information The online version contains supplementary material available at https://doi.org/10.1007/s10340-025-01874-6.

Acknowledgements We thank the East Malling Trust for their support and AHDB TF233 project for the collection of spray records and pest monitoring data. Thanks to pcfruit for providing the R script used for both the pear psyllid phenology model and earwig degree day model.

Author contributions Laura Reeves, Michael Garratt, Michelle Fountain and Deepa Senapathi conceived and designed the study. Tim Belien provided R code for the pear psyllid phenology model and earwig degree day model and insights into their use. Laura Reeves carried out data analyses and drafted the manuscript with all authors providing feedback on multiple drafts prior to submission.

Funding This project was funded by BBSRC (BB/V509747/1) and Waitrose Agronomy Group as part of the Waitrose Collaborative Training Partnership.

Data availability Dataset is accessible from the University of Reading Research Data Archive.

Declarations

Competing interests The authors declare that they have no known competing financial interests or personal relationships that could influence the work reported in this paper.

References

Amano T, Smithers RJ, Sparks TH, Sutherland WJ (2010) A 250-year index of first flowering dates and its response to temperature changes. Proc R Soc B 277(1693):2451–2457. https://doi.org/10.1098/rspb.2010.0291

Anderson J, Richardson E, Kesner C (1985) Validation of chill unit and flower bud phenology models for "Montmorency" sour cherry. Acta Hortic 184:71–78. https://doi.org/10.17660/ActaHortic.1986.184.7

Atkinson C, Brennan R, Jones H (2013) Declining chilling and its impact on temperate perennial crops. Environ Exp Bot 91:48–62. https://doi.org/10.1016/j.envexpbot.2013.02.004

Atkinson C, Sunley R, Jones H, Brennan R, Darby P (2004) Winter chill in fruit. Defra Report, CTC, 206

Auffret AG (2021) Historical floras reflect broad shifts in flowering phenology in response to a warming climate. Ecosphere 12(7):e03683. https://doi.org/10.1002/ecs2.3683

Belien T, Moerkens R, Leirs H, Peusens G (2012) Earwig Management Tool: a practical software application to predict and optimize the development of earwig populations in pip fruit orchards. Commun Agric Appl Biol Sci 77(4):657–662. https://doi.org/10.5555/20133110048

Belien T, Moerkens R, Leirs H, Peusens G, Bylemans D (2013) "Earwig management tool": transferring knowledge of population dynamics and side effects on earwigs (*Forficula auricularia* L.). IOBC Bull 91:411–418

Belien T, Bangels E, Brenard N, Reijniers J, Leirs H, Bylemans D (2017) Optimized timing of IPM treatments against pear psylla (Cacopsylla pyri) based on a temperature driven population dynamics model. IOBC 123:96–100. https://doi.org/10.5555/20173367427

Bonte J, De Ro M, Conlong D, De Clercq P (2012) Thermal biology of the predatory bugs *Orius thripoborus* and *O. naivashae* (Hemiptera: Anthocoridae). Environ Entomol 41(4):989–996. https://doi.org/10.1603/EN12089

Carraro L, Loi N, Ermacora P (2001) The "life cycle" of pear decline phytoplasma in the vector *Cacopsylla pyri*. Plant Pathol J 83:87–90. https://www.jstor.org/stable/41998044

CEDA (2023) MIDAS Open: UK daily temperature data. https://data.ceda.ac.uk/badc/ukmo-midas-open/data/uk-daily-temperature-obs/dataset-version-202308/kent/00744_east-malling/qc-version-1 Accessed December 7 2023

Cesaraccio C, Spano D, Snyder RL, Duce P (2004) Chilling and forcing model to predict bud-burst of crop and forest species. Agric for Meteorol 126(1–2):1–13. https://doi.org/10.1016/j.agrformet.2004.03.002

Chang JF (1977) Studies on the susceptibility of pear trees to pear psylla, *Psylla pyricola* Foerster (Homoptera: Psyllidae). Diss Abstr Int 45:3013. https://doi.org/10.20381/ruor-8518

Civolani S, Pasqualini E (2003) *Cacopsylla pyri* L. (Hom., Psyllidae) and its predators relationship in Italy's Emilia-Romagna Region. J Entomol 127:214–220. https://doi.org/10.1046/j.1439-0418.2003.00737.x

Civolani S, Soroker V, Cooper WR, Horton DR (2023) Diversity, biology, and management of the pear psyllids: a global look. Ann Entomol Soc Am 116(6):331–357. https://doi.org/10.1093/aesa/saad025

Cross J, Berrie A (2003) Integrated pest and disease management in pear production. In: Best practice guide for UK pear production. IOBC Bull, vol 29(1), pp 129–138

Damien M, Tougeron K (2019) Prey–predator phenological mismatch under climate change. Curr Opin Insect Sci 35:60–68. https://doi.org/10.1016/j.cois.2019.07.002

Daniel C, Pfammatter W, Kehrli P, Wyss E (2005) Processed kaolin as an alternative insecticide against the European pear sucker, *Cacopsylla pyri* (L.). J Appl Entomol 129(7):363–367. https://doi.org/10.1111/j.1439-0418.2005.00981.x

Defra (2023) Latest horticulture statistics. https://www.gov.uk/government/statistics/latest-horticulture-statistics Acessed November 14 2023

Derksen R, Vitanza S, Welty C, Miller S, Bennett M, Zhu H (2007) Field evaluation of application variables and plant density for bell pepper pest management. J ASABE Trans 50(6):1945–1953. https://doi.org/10.13031/2013.24090

Van den Dool K (2006) Evaporative cooling of apple and pear orchards. Dissertation, University of Stellenbosch.

Drepper B, Gobin A, Remy S, Van Orshoven J (2020) Comparing apple and pear phenology and model performance: what seven decades of observations reveal. Agronomy 10(1):73. https://doi.org/10.3390/agronomy10010073

DuPont ST, Strohm C (2020) Integrated pest management programmes increase natural enemies of pear psylla in Central Washington pear orchards. J Appl Entomol 144(1–2):109–122. https://doi.org/10.1111/jen.12694

DuPont ST, Strohm C, Nottingham L, Rendon D (2021) Evaluation of an integrated pest management program for central Washington pear orchards. Biol Control 152:104390. https://doi.org/10.1016/j.biocontrol.2020.104390

DuPont ST, Strohm C, Kogan C, Hilton R, Nottingham L, Orpet R (2023) Pear psylla and natural enemy thresholds for successful integrated pest management in pears. J Econ Entomol 116(4):1249–1260. https://doi.org/10.1093/jee/toad101

Erler F (2004) Natural enemies of the pear psylla *Cacopsylla pyri* in treated vs untreated pear orchards in Antalya, Turkey. Phytoparasitica 32(3):295–304. https://doi.org/10.1007/BF02979824

Erler F, Cetin H (2007) Effect of kaolin particle film treatment on winterform oviposition of the pear psylla *Cacopsylla pyri*. Phytoparasitica 35:466–473. https://doi.org/10.1007/BF03020605

Fadón E, Espiau MT, Errea P, Alonso Segura JM, Rodrigo J (2023) Agroclimatic requirements of traditional European pear (*Pyrus communis* L.) cultivars from Australia, Europe, and North America. Agronomy 13(2):518. https://doi.org/10.3390/agronomy13020518

FAOSTAT (2022) Crops and livestock products. https://www.fao.org/faostat/en/#data/QCL Accessed 9 November 2023

Fernandez E, Schiffers K, Urbach C, Luedeling E (2022) Unusually warm winter seasons may compromise the performance of current phenology models–Predicting bloom dates in young apple trees with PhenoFlex. Agric for Meteorol 322:109020. https://doi.org/10.1016/j.agrformet.2022.109020

Fields G, Beirne B (1973) Ecology of anthocorid (Hemiptera: Anthocoridae) predators of the pear psylla (Homoptera: Psyllidae) in the Okanagan Valley, British Columbia. J Entomol Soc B C 70:18–19. https://journal.entsocbc.ca/index.php/journal/article/view/1825

Fishman S, Erez A, Couvillon G (1987) The temperature dependence of dormancy breaking in plants: computer simulation of processes studied under controlled temperatures. J Theor Biol 126(3):309–321. https://doi.org/10.1016/S0022-5193(87)80237-0

Fitter A, Fitter R (2002) Rapid changes in flowering time in British plants. Science 296(5573):1689–1691. https://doi.org/10.1126/science.1071617

Fountain M, Nagy C, Harris A, Cross J (2013) Importance of naturally occurring predators for pear sucker control. In: IOBC Bulletin, vol 91, pp 117–125

Gobin B, Peusens G, Moerkens R, Leirs H (2008) Understanding earwig phenology in top fruit orchards. Ecofruit 13:208–212. https://doi.org/10.5555/20113407038

Harries F, Burts EC (1965) Insecticide resistance in the pear psylla. J Econ Entomol 58(1):172–173. https://doi.org/10.1093/jee/58.1.172

Harrington R, Woiwod I, Sparks T (1999) Climate change and trophic interactions. Trends Ecol Evol 14(4):146–150. https://doi.org/10.1016/S0169-5347(99)01604-3

Helsen H, Vaal F, Blommers L (1998) Phenology of the common earwig *Forficula auricularia* L. (Dermaptera: Forficulidae) in an apple orchard. Int J Pest Manag 44(2):75–79. https://doi.org/10.1080/096708798228356

Horton DR (1999) Monitoring of pear psylla for pest management decisions and research. J Integr Pest Manag 4(1):1–20. https://doi.org/10.1023/A:1009602513263

Horton DR (2024) Psyllids in natural habitats as alternative resources for key natural enemies of the pear psyllids (Hemiptera:

Psylloidea). InSects 15(1):37. https://doi.org/10.3390/insects15010037

Jenser G, Szita E, Balint J (2010) Measuring pear psylla population density (*Cacopsylla pyri* L. and *C. pyricola Förster*): review of previous methods and evaluation of a new technique. North-West J Zool 6(1):54. https://biozoojournals.ro/nwjz/content/v6.1/nwjz.061106.Jenser.pdf

Ju RT, Gao L, Wei SJ, Li B (2017) Spring warming increases the abundance of an invasive specialist insect: links to phenology and life history. Sci Rep 7(1):14805. https://doi.org/10.1038/s41598-017-14989-3

Kapatos E, Stratopoulou E (1999) Duration times of the immature stages of *Cacopsylla pyri* L. (Hom., Psyllidae), estimated under field conditions, and their relationship to ambient temperature. J Appl Entomol 123(9):555–559. https://doi.org/10.1046/j.1439-0418.1999.00417.x

Karuppaiah V, Sujayanad G (2012) Impact of climate change on population dynamics of insect pests. World J Agric Sci 8(3):240–246. https://doi.org/10.5555/20123362574

Kölliker M (2007) Benefits and costs of earwig (*Forficula auricularia*) family life. Behav Ecol Sociobiol 61:1489–1497. https://doi.org/10.1007/s00265-007-0381-7

Kucerová J, Talacko L, Lauterer P, Navratil M, Fialová R (2007) Molecular tests to determine *Candidatus Phytoplasma pyri* presence in psyllid vectors from a pear tree orchard in the Czech Republic–a preliminary report. Bull Insectology 60(2):191–192. https://doi.org/10.5555/20073295351

Lame RJ (1974) Earwig travel in relation to habitat. University of British Columbia. Dissertation. https://doi.org/10.14288/1.0100004

Lee H, Kang WS, Ahn MI, Cho K, Lee JH (2016) Predicting temporal shifts in the spring occurrence of overwintered *Scotinophara lurida* (Hemiptera: Pentatomidae) and rice phenology in Korea with climate change. Int J Biometeorol 60:53–61. https://doi.org/10.1007/s00484-015-1004-z

Lenfant C, Lyoussoufi A, Chen X, D'Arcier FF, Sauphanor B (1994) Potentialités prédatrices de *Forficula auricularia* sur le psylle du poirier *Cacopsylla pyri*. Entomol Exp Appl 73(1):51–60. https://doi.org/10.1111/j.1570-7458.1994.tb01838.x

Lordan J, Alegre S, Moerkens R, Sarasúa MJ, Alins G (2015) Phenology and interspecific association of *Forficula auricularia* and *Forficula pubescens* in apple orchards. Span J Agric Res 13(1):1003. https://doi.org/10.5424/sjar/2015131-6814

Lowe JA, Bernie D, Bett P, Bricheno L, Brown S, Calvert D, Clark R, Eagle K, Edwards T, Fosser G (2018) UKCP18 science overview report. https://www.researchgate.net/profile/Stephen-E-Belcher/publication/345815169_UKCP18-Overview-report/links/5faed14aa6fdcc9ae04dc04e/UKCP18-Overview-report.pdf Accessed 24 April 2024

Luedeling E, Schiffers K, Fohrmann T, Urbach C (2021) PhenoFlex-an integrated model to predict spring phenology in temperate fruit trees. Agric for Meteorol 307:108491. https://doi.org/10.1016/j.agrformet.2021.108491

Luedeling E (2023) ChillR: Statistical Methods for Phenology Analysis in Temperate Fruit Trees, R package version 0.75.

Luedeling E (2024) Tree phenology analysis with R. https://inresgb-lehre.iaas.uni-bonn.de/chillR_book/introduction.html Accessed 24 April 2024

Lyoussoufi A, Gadenne C, Rieux R, D'Arcier F F (1994) Évolution de la diapause du psylle du poirier Cacopsylla pyri dans les conditions naturelles. Entomol Exp Appl 70(2):193–199. https://doi.org/10.1111/j.1570-7458.1994.tb00747.x

Martínez-García H, Aragón-Sánchez M, Sáenz-Romo MG, Román-Fernández LR, Veas-Bernal A, Marco-Mancebón VS, Pérez-Moreno I (2018) Mathematical models for predicting development of *Orius majusculus* (Heteroptera: Anthocoridae) and its applicability to biological control. J Econ Entomol 111(4):1904–1914. https://doi.org/10.1093/jee/toy127

Mauck KE, Gebiola M, Percy DM (2024) The hidden secrets of Psylloidea: biology, behavior, symbionts, and ecology. Annu Rev Entomol 69:277–302. https://doi.org/10.1146/annurev-ento-120120-114738

McMullen R, Jong C (1977) Effect of temperature on developmental rate and fecundity of the pear psylla, *Psylla pyricola* (Homoptera: Psyllidae). Can Entomol 109(2):165–169. https://doi.org/10.4039/Ent109165-2

MetOffice (2018) UKCP18 Guidance: Representative Concentration Pathways. https://www.metoffice.gov.uk/binaries/content/assets/metofficegovuk/pdf/research/ukcp/ukcp18-guidance---representative-concentration-pathways.pdf Accessed 19 November 2023

MetOffice (2022) UK Climate Projections: Headline Findings. https://www.metoffice.gov.uk/binaries/content/assets/metofficegovuk/pdf/research/ukcp/ukcp18_headline_findings_v4_aug22.pdf Accessed 19 November 2023

Moerkens R, Gobin B, Peusens G, Helsen H, Hilton R, Dib H, Suckling DM, Leirs H (2011) Optimizing biocontrol using phenological day degree models: the European earwig in pipfruit orchards. Agric for Entomol 13(3):301–312. https://doi.org/10.1111/j.1461-9563.2011.00525.x

Moorthy PK, Kumar NK (2004) Integrated pest management in vegetable crops. Indian Agric 2:95. https://www.researchgate.net/publication/352257410_Integrated_pest_management_in_vegetable_crops

Murphy J, Harris G, Sexton D, Kendon E, Bett P, Clark R, Yamazaki K (2018) UKCP18 land projections: Science report. Met Office Hadley Centre. https://www.rmets.org/sites/default/files/2019-02/UKCP18_LandProjections_James%20Murphy.pdf Accessed 20 April 2024

Næss ETL (2016) Molecular analysis of predation by anthocorid bugs on the pear psyllid *Cacopsylla pyri* (Homoptera, Psyllidae). Norwegian University of Life Sciences. Dissertation.

Nagy C, Cross J, Luton M, Ashdown C (2008) Mixed deciduous hedgerows as sources of anthocorids and other predators of pear psyllids in the UK. IOBC 7:395–401. https://iobc-wprs.org/product/mixed-deciduous-hedgerows-as-sources-of-anthocorids-and-other-predators-of-pear-psyllidin-the-uk/

Neven LG (2000) Physiological responses of insects to heat. Postharvest Biol Technol 21(1):103–111. https://doi.org/10.1016/S0925-5214(00)00169-1

Nottingham LB, Beers EH (2020) Management of pear psylla (Hemiptera: Psyllidae) using reflective plastic mulch. J Econ Entomol 113(6):2840–2849. https://doi.org/10.1093/jee/toaa241

Oz V, Erler F (2021) Evaluation of oviposition deterrent activity of four oily substances against winterform females of pear psylla, Cacopsylla pyri. Bull Insect 74(2):285–290. https://doi.org/10.5555/20220236870

Pasqualini E, Civolani S, Grappadelli LC (2002) Particle film technology: approach for a biorational controlof *Cacopsylla pyri* (Rhynchota Psyllidae) in Northern Italy. Bull Insectology 55(1–2):39–42. https://doi.org/10.5555/20033033231

Petrakova L, Michalko R, Loverre P, Sentenska L, Korenko S, Pekar S (2016) Intraguild predation among spiders and their effect on the pear psylla during winter. Agric Ecosyst Environ 233:67–74. https://doi.org/10.1016/j.agee.2016.08.008

Prodanović DJ, Protic L, Mlhajlović L (2010) Predators and parasitoids of *Cacopsylla pyri* (L.) (Hemiptera: Psyllidae) in Serbia. Pesticidi i Fitomedicina 25(1):29–42. https://doi.org/10.2298/PIF1001029J

Reeves LA, Garratt MP, Fountain MT, Senapathi D (2022) Climate induced phenological shifts in pears–a crop of economic importance in the UK. Agric Ecosyst Environ 338:108109. https://doi.org/10.1016/j.agee.2022.108109

Reeves LA, Garratt MP, Fountain MT, Senapathi D (2023) Functional and behavioral responses of the natural enemy *Anthocoris nemoralis* to *Cacopsylla pyri*, at different temperatures. J Insect Behav 36(3):222–238. https://doi.org/10.1007/s10905-023-09836-5

Reeves LA, Garratt MP, Fountain MT, Senapathi D (2024) A whole ecosystem approach to pear psyllid (*Cacopsylla pyri*) management in a changing climate. J Pest Sci 97:1203–1226. https://doi.org/10.1007/s10340-024-01772-3

Renner SS, Zohner CM (2018) Climate change and phenological mismatch in trophic interactions among plants, insects, and vertebrates. Annu Rev Ecol Evol Syst 49:165–182. https://doi.org/10.1146/annurev-ecolsys-110617-062535

Sansavini S, Musacchi S (2000) European pear orchard design and HDP management: a review. In: VIII International Symposium on Pear, vol 596, pp 589–601

Saour G, Ismail H, Hashem A (2010) Impact of kaolin particle film, spirodiclofen acaricide, harpin protein, and an organic biostimulant on pear psylla *Cacopsylla pyri* (Hemiptera: Psyllidae). Int J Pest Manag 56(1):75–79. https://doi.org/10.1080/09670870903156632

Schaub L, Graf B, Butturini A (2005) Phenological model of pear psylla *Cacopsylla pyri*. Entomol Exp Appl 117(2):105–111. https://doi.org/10.1111/j.1570-7458.2005.00339.x

Schwalm CR, Glendon S, Duffy PB (2020) RCP8. 5 tracks cumulative CO2 emissions. Proc Natl Acad Sci 117(33):19656–19657. https://doi.org/10.1073/pnas.2007117117

Scutareanu P, Lingeman R, Drukker B, Sabelis MW (1999) Cross-correlation analysis of fluctuations in local populations of pear psyllids and anthocorid bugs. Ecol Entomol 24(3):354–363. https://doi.org/10.1046/j.1365-2311.1999.00199.x

Sek Kocourek F, Stará J (2006) Management and control of insecticide-resistant pear psylla (*Cacopsylla pyri*). J Fruit Ornam Plant Res 14(3):167–174

Shaw B, Nagy C, Fountain MT (2021) Organic control strategies for use in IPM of invertebrate pests in apple and pear orchards. InSects 12(12):1106. https://doi.org/10.3390/insects12121106

Sigsgaard L (2010) Habitat and prey preferences of the two predatory bugs *Anthocoris nemorum* (L.) and *A. nemoralis* (Fabricius) (Anthocoridae: Hemiptera-Heteroptera). Biol Control 53(1):46–54. https://doi.org/10.1016/j.biocontrol.2009.11.005

Solomon M, Cranham J, Easterbrook M, Fitzgerald J (1989) Control of the pear psyllid, *Cacopsylla pyricola*, in south east England by predators and pesticides. Crop Prot 8(3):197–205. https://doi.org/10.1016/0261-2194(89)90027-6

Sparks T, Croxton P, Collinson N, Taylor P (2005) Examples of phenological change, past and present, UK Farming. Ann Appl Biol 146(4):531–537. https://doi.org/10.1111/j.1744-7348.2005.050016.x

Stoeckli S, Hirschi M, Spirig C, Calanca P, Rotach MW, Samietz J (2012) Impact of climate change on voltinism and prospective diapause induction of a global pest insect–*Cydia pomonella* (L.). PLoS ONE 7(4):e35723. https://doi.org/10.1371/journal.pone.0035723

Stratopoulou E, Kapatos E (1992) Phenology of population of immature stages of pear psylla, *Cαcopsyllα pyri*, in the region of magnesia (Greece). Entomol Hell 10:11–17. https://doi.org/10.12681/eh.13998

Suckling D, Burnip G, Hackett J, Daly J (2006) Frass sampling and baiting indicate European earwig (*Forficula auricularia*) foraging in orchards. J Appl Entomol 130(5):263–267. https://doi.org/10.1111/j.1439-0418.2006.01064.x

Süle S, Jenser G, Szita E, Bertaccini A, Maini S (2007) Management of pear decline caused by '*Candidatus* Phytoplasma pyri' in Hungary. Bull Insectology 60(2):319–320. https://doi.org/10.5555/20073295409

Tougeron K, Iltis C, Renoz F, Albittar L, Hance T, Demeter S, Le Goff GJ (2021) Ecology and biology of the parasitoid *Trechnites insidiosus* and its potential for biological control of pear psyllids. Pest Manag Sci 77(11):4836–4847. https://doi.org/10.1002/ps.6517

Tsallis C, Stariolo DA (1996) Generalized simulated annealing. Physica A. Stat 233(1–2):395–406. https://doi.org/10.1016/S0378-4371(96)00271-3

UKCP (2021) UK Climate Projections User Interface Data: Variables from global projections (60km) over UK for daily data. https://ukclimateprojections-ui.metoffice.gov.uk/products/form/LS2_Subset_02 Accessed 10 January 2024

Van Vuuren DP, Stehfest E, Den Elzen MG, Kram T, Van Vliet J, Deetman S, Isaac M, Klein Goldewijk K, Hof A, Mendoza Beltran A (2011) RCP2. 6: exploring the possibility to keep global mean temperature increase below 2 C. Clim Change 109:95–116. https://doi.org/10.1007/s10584-011-0152-3

Vrancken K, Trekels H, Thys T, Belian T, Bylemans D, Demaeght P, Van Leeuwen T, De Clercq P (2014) The presence of beneficial arthropods in organic versus IPM pear orchards and their ability to predate pear suckers (*Cacopsylla pyri*). ISHS, vol 1094, pp 427–429. https://doi.org/10.17660/ActaHortic.2015.1094.55

Wyver C, Potts SG, Edwards R, Edwards M, Senapathi D (2023) Climate driven shifts in the synchrony of apple (*Malus* x *domestica Borkh*) flowering and pollinating bee flight phenology. Agric for Meteorol 329:109281. https://doi.org/10.1016/j.agrformet.2022.109281

Wyver C, Potts SG, Pitts R, Riley M, Janetzko G, Senapathi D (2024) New citizen science initiative enhances flowering onset predictions for fruit trees in Great Britain. Hortic Res 11(6):122. https://doi.org/10.1093/hr/uhae122

Xiang Y, Gubian S, Suomela B, Hoeng J (2013) Generalized simulated annealing for global optimization: the GenSA package. R J 5(1):13

Yanik E, Unlu L (2011) Influences of temperature and humidity on the life history parameters and prey consumption of *Anthocoris minki* Dohrn (Heteroptera: Anthocoridae). Appl Entomol Zool 46:177–184. https://doi.org/10.1007/s13355-011-0029-y